**Stress-Density Relationships for an Agricultural Soil**

by

Vasilis Parathiras

Thesis submitted to the Faculty of the

Virginia Polytechnic Institute and State University

in partial fulfillment of the requirements for the degree of

Masters of Science

in

Mechanical Engineering

APPROVED:

H. H. Robertshaw, Chairman

J. V. Perumpral

R. H. Fries

April, 1987

Blacksburg, Virginia

**Stress-Density Relationships for an Agricultural Soil**

by

Vasilis Parathiras

Committee Chairman: H. H. Robertshaw

Mechanical Engineering

(ABSTRACT)

Triaxial tests under high loading rates and different confining pressures simulate the multi-pass effect of a tractor wheel loading on the soil. A volume measuring technique was developed to be used in triaxial tests conducted under high loading rates.

A sandy clay agricultural soil was tested under predetermined conditions using an INSTRON loading frame, a differential pressure transducer and an APPLE II + microcomputer. A preliminary analysis indicated that the measuring technique that was developed, was capable of recording volume changes under high loading rates. Stress-density plots were created using the obtained data and a mathematical model was developed relating stress to density. Stress-strain data was used to evaluate the soil parameters under the Mohr-Coulomb failure criteria. Furthermore, the influence of the initial soil density on the soil behavior was evaluated and subsequently compared to the results of a similar study conducted under a different initial density.

## Acknowledgements

I would like to express my gratitude to Dr. J. V. Perumpral for his support and guidance throughout this study. Appreciation is also extended to Dr. H. H. Robertshaw and Dr. R. H. Fries for their suggestions and assistance.

Thanks to Dr. K. Diehl for the use of his laboratory and his help during the initial setup of the testing facility. Also, special thanks to Mr. Z. Agioutantis for his help with the computer aspects of this study and his suggestions during the analysis and processing of the results.

Finally, deepest appreciation is extended to my parents for their love and support during my university career.

# Table of Contents

# List of Illustrations

## List of Symbols

| | | |
|---|---|---|
| BWV | = | Bulk Weight Volume |
| $\sigma_{mean}$ | = | mean normal stress |
| $\sigma_1, \sigma_2, \sigma_3$ | = | principal stresses |
| $\tau_{max}$ | = | maximum shear stress |
| e | = | void ratio |
| $\varphi$ | = | angle of internal friction |
| c | = | cohesion |
| E | = | modulus of elasticity |
| $\nu$ | = | Poisson's ratio |

# Chapter 1

## *Introduction*

The evolution of the tractor played a significant part in the change of farming technology, farm sizes, and production. Although the total number of farms has declined from 5,648,000 in 1950 to 2,752,000 in 1980, the average size of a farm in the U.S. has increased from 213 acres in 1950 to 393 acres in 1980 and the average yield has increased by 58% in the same period. During this period the productivity has also increased, since the number of man-hours needed to cultivate an acre of wheat was reduced from 7.4 hours in 1940 to 2.9 hours in 1970. This reduction in labor requirement resulted from the mechanization of farming operations, which is reflected in an increase in tractor units, from 920,000 in 1930, to over 4,450,000 in 1970.

With the increase in farm size the size of the tractor also increased. Today's agricultural tractor is a more complex vehicle, larger in size and weight, used to propel and power a large variety of implements for agricultural production. The average weight of a tractor, which is the main cause for the soil compaction, has also increased from 1.4 tons in 1968, to 6.8 tons in 1983. The result is a stronger soil with reduced hydraulic conductivity, high root impedance, and decreased water and nutrient storage capacity, which are not desirable for plant growth. On the other hand,

this compacted soil is considered a desirable feature in construction applications such as roads, dams, and building foundations, because soil compaction results in increased soil strength.

Either for increasing or minimizing soil compaction, one should be able to predict the soil responses to boundary loads. Thus, a clear understanding of the mechanics of soil compaction is essential, and experimental and analytical methods have been applied for that purpose. The experimental procedures available are time consuming, labor intensive, and expensive. On the other hand, if analytical procedures such as the finite element method, are developed and are available, the soil compaction process could be understood more clearly with minimum number of experiments.

Pollock (1983), conducted a feasibility study and demonstrated the potential use of the finite element method for predicting the multi-pass effect of vehicles in soil compaction. Since appropriate constitutive relationships for agricultural soils were not available, this study was performed using constitutive relationships already available for pure sand and clay to develop volumetric strain contours. This study concluded that the finite element method can be effectively used to study the soil behavior under vehicle loading. In order to achieve more realistic predictions of soil compaction, however, appropriate stress-strain or stress-density relationships for the particular soil under consideration are necessary.

An investigation completed recently developed constitutive relationships for two agricultural soils (Brandon, 1987). While these models are suitable for finite element analysis and can be applied in order to obtain information on stress and strain within the soil due to tractor loading, they can not be used to predict the soil density changes. Therefore, the overall objective of this study is to develop a suitable device

to measure volume changes of the soil during high loading rates, in order to obtain stress-density relationships necessary to complement the existing soil compaction models.

## *Objectives*

The specific objectives of this study are:

- To develop a technique for recording the sample volume change during triaxial tests at high loading rates.

- To develop a stress-density relationship for an agricultural soil.

- To collect additional data to further improve the model developed by Brandon (1987).

# Chapter 2

## *Literature Review*

### 2.1 Compaction Models

Soil compaction is generally expressed in terms of change in pore-space, void ratio, dry volume weight ($\gamma_d$), and bulk weight volume (BWV) defined as ($\frac{1}{\gamma_d}$). Various models have been developed to relate the applied stress to the soil volume change and are discussed below.

Soehne (1958) studied the compaction by using a piston to load soil in a cylindrical container. The test cylinders, 28 cm in outside diameter, 13 cm in height with a volume of 10,000 cc, where filled with unsaturated and loose soil that was strained uniaxially. The model is based on the assumption that the compaction phenomena were unequally controlled by the major principal stress ($\sigma_1$) and that the amount of compaction was linearly related to the logarithm of the major principal stress. Small lead spheres placed in the soil were used to observe the compaction pattern with the use of x-ray techniques. It was reported that lines of equal principal stresses were observed, at some distance from the piston. In addition these lines appeared to coincide with the lines of equal compaction.

VandenBerg (1966) used the triaxial test to develop a model correlating the bulk density, the shearing strain and the mean normal stress. The developed function was:

$$BWV = \sigma_{mean}(1 + \bar{\gamma}_{max}) \qquad [1]$$

where,

BWV = Bulk Weight Volume;

$\sigma_{mean}$ = mean normal stress;

$\bar{\gamma}_{max}$ = shearing strain for all loading sequences.

The model was developed using the experimental results for Lloyd, Hiwassee, Congaree, and Huston clays. It is suggested, however, that more experiments, under varying conditions, are needed to evaluate the loading characteristics of the clays.

Bailey and VandenBerg (1968) developed a mathematical model correlating the Bulk Weight Volume to compaction and shear. They used four different soil types on a triaxial test with loose, unsaturated samples and constant moisture levels. A three dimensional yield diagram was developed using the Bulk Weight Volume, maximum shearing stress and mean normal stress as coordinate axes. The mathematical equation derived from these experiments is given below:

$$BWV = m \log \zeta + n\left[\frac{\tau_{max}}{\sigma_{mean}}\right] + \beta \qquad [2]$$

where,

BWV = Bulk Weight Volume;

$\zeta = \sqrt{\sigma^2_{mean} + \tau^2_{max}}$ ;

$\sigma_{mean}$ = mean normal stress;

$\tau_{max}$ = maximum shear stress;

m, n, $\beta$ = are soil parameters.

Dunlap and Weber (1971) investigated the compaction of the soil under a general state of stress. Triaxial tests were conducted on low density, rectangular - paralleloppiped shaped soil samples. The main advantage of the non-circular soil sample was that the principal stresses could be varied independently, which is not possible with the standard triaxial test soil sample. By compacting the samples at different levels, it was concluded that compaction was maximum when $\sigma_2 = \sigma_3$ and minimum when $\sigma_2 = \sigma_1$, under fixed principal stresses. A set of curves was subsequently developed to represent shearing stress versus bulk weight volume at any level of mean stress. The following function was subsequently proposed to correlate shearing stress and Bulk Weight Volume:

$$BWV = M \ \ln(\sigma_{mean}) + N - \frac{\tau_{max} - (1 - A)S_y}{AG} \qquad [3]$$

where,

M,N are determined from the soil loading curves;

G,AG are the slopes of the loading curve (initial, final);

$S_y$ = $\tau_{max}$ at the yield point;

A = 1 when $0 \leq \tau_{max} \leq S_y$;

$A = \frac{AG}{G}$ = constant when $S_y \leq \tau_{max}$

Koolen (1974) uniaxially compacted Wageningen silt clay and Lexkesveer loam at varying moisture contents. The compaction response was characterized by the void ratio (e) that was defined as the total volume of pores divided by the total volume of solids. The results indicated a hyperbolic relationship between void ratio and pressure given by:

$$\frac{e - e_f}{e_1 - e_f} = \frac{1}{1 + \left[\frac{\sigma_1}{c}\right]} \qquad [4]$$

where,

$e_1$ = theoretical initial void ratio;

$e$ = void ratio of $\sigma_1$;

$e_f$ = theoretical final void ratio;

$c$ = stress level that gave an average void ratio between $e_1$ and $e_f$ referred to as median stress, and;

$\sigma_1$ = major principal stress.

The proposed equation [4] describes poorly the experimentally observed soil reaction at low confining pressures, because of the different initial soil condition created when filling the confined uniaxial cylinder. Poor description was also observed at high pressures (above 350 kPa) and was reasoned to be a result of non-uniform stress distribution in the test cylinder caused by water being forced out of the soil.

Kumar and Weber (1974) used right square prismatic samples of soil in a triaxial test to study the compaction of Lloyd clay with 19% moisture content under different load paths. It was concluded that the volume change produced by the deviatoric stress at any level or mean stress, $\sigma_{mean}$, did not relate uniquely to either $\tau_{max}$ or $\tau_{octahedral}$. However, it was found that a new parameter, $\tau_{compacted}$, related uniquely with the volume change, by the relationship:

$$\text{Volume change} = m\ \tau_{compacted} \qquad [5]$$

where,

$$m = 11.5\,(\sigma_{mean})^{-0.957}\ ;$$

$$\tau_{compacted} = \frac{\sigma_1 - \sigma_3}{2} + 0.5\,\frac{\sigma_1 - \sigma_2}{2}$$

It was also determined that $\tau_{compacted}$ is independent from the deviatoric stress path, and that when the deviatoric stress is removed and then reapplied along the original stress path there is an increase in volume.

Amir *et al.* (1976) developed a logarithmic model to predict the change in soil volume due to pressure, based on the assumption that soil compaction is mainly affected by the pressure applied by the machinery and the ambient soil moisture content. According to them the soil porosity (n) can be expressed as:

$$n = A_n - B_n \times \ln(\sigma_r + \sigma) - c_n \times \ln \varphi \qquad [6]$$

where,

$n$ = total volume of pores/volume of soil, %;

$\sigma_r$ = residual pressure;

$\sigma$ = pressure applied;

$\varphi$ = volumetric soil moisture content, %, and;

$A_n$, $B_n$, $C_n$ = soil parameters.

The practical use of the proposed model was demonstrated by determining the extra amount of compaction caused by a tractive device when the moisture content of the soil was changed.

Larson *et al.* (1980) derived relationships between bulk density, moisture content and principal stress for 36 different agricultural soils. Their experimental results indicated that there was a linear relationship between the bulk density and the logarithm of the applied principal stress ($\sigma_1$) for a specific moisture content. Additionally, the curves

relating bulk density and log ($\sigma_1$) for different moisture contents were parallel to each other. The slope of the proposed curves was found to depend on the clay content. The proposed relationship that was derived from the results on confined uniaxial compression tests is:

$$P = [P_k + \Delta(t) \times (s_1 - s_k)] + CI \times \log(\frac{\sigma_a}{\sigma_k}) \quad [7]$$

where,

P = compacted bulk density at corresponding applied stress (gr/cc);

$P_k$ = bulk density at a known stress (gr/cc);

$\sigma_a$ = current applied stress, kPa;

$\sigma_k$ = known stress level, kPa;

$s_1$ = desired degree of saturation, %;

$s_k$ = degree of saturation at $P_k$ and $\sigma_k$, %;

$\Delta(t)$ = slope of the curve representing bulk density versus degree of saturation at $\sigma_k$, and;

CI = compression index.

Koolen and Kuipers (1983) developed a general model to describe the rapid soil compaction. A function, f, was proposed to relate the stress to the strain and can be determined through triaxial tests conducted for a single load cycle with the following assumptions:

1. Volume expressed as bulk weight volume (BWV) will be changing.
2. The soil is loose when first loaded.
3. $\sigma_2 = \sigma_3$
4. Loading is rapid enough to prevent water movement.

5. The principal loading directions are kept constant.

Based on these assumptions, they suggested that the BWV can be calculated for a particular $\sigma_1$ and $\sigma_3$ combination and can be expressed as:

$$BWV = f(\sigma_1, \sigma_3) \quad [8]$$

Since $\sigma_{mean}$ and $\tau_{max}$ are functions of $\sigma_1, \sigma_3$ the same relationship can also be expressed as:

$$BWV = F(\sigma_{mean}, \tau_{max}) \quad [9]$$

The functions F, f are generally determined through a series of triaxial tests conducted at different stress conditions. Figure 1 shows a three dimensional representation of F and f. Function F is a surface bounded by lines CD and AB. The curve CD represents all critical states of a certain soil obtained by keeping the ratio $\frac{\tau_{max}}{\sigma_{mean}}$ constant. Curve AB, on the other hand, is the equal distortion line of the samples, created by keeping $\sigma_1 = \sigma_3$. Loading during agricultural operations may create stress conditions somewhere between curves GH and CD.

Function f is included between curves AC and AB. Curve AB represents the tests conducted under equal compression from all directions ($\sigma_1 = \sigma_3$). Curve AC represents the critical states and is created by keeping the ratio $\frac{\sigma_3}{\sigma_1}$ constant. The models developed by Bailey and VandenBerg (1963) and Dunlap and Weber (1971) for Lloyd clays were applied for various $\frac{\sigma_3}{\sigma_1}$ ratios, under the assumption that BWV changes mainly with $\sigma_1$ and very little with $\sigma_3$. It was concluded that $\sigma_3$ has a small influence on the change of BWV (Figure 2). Consequently a triaxial test is not needed to de-

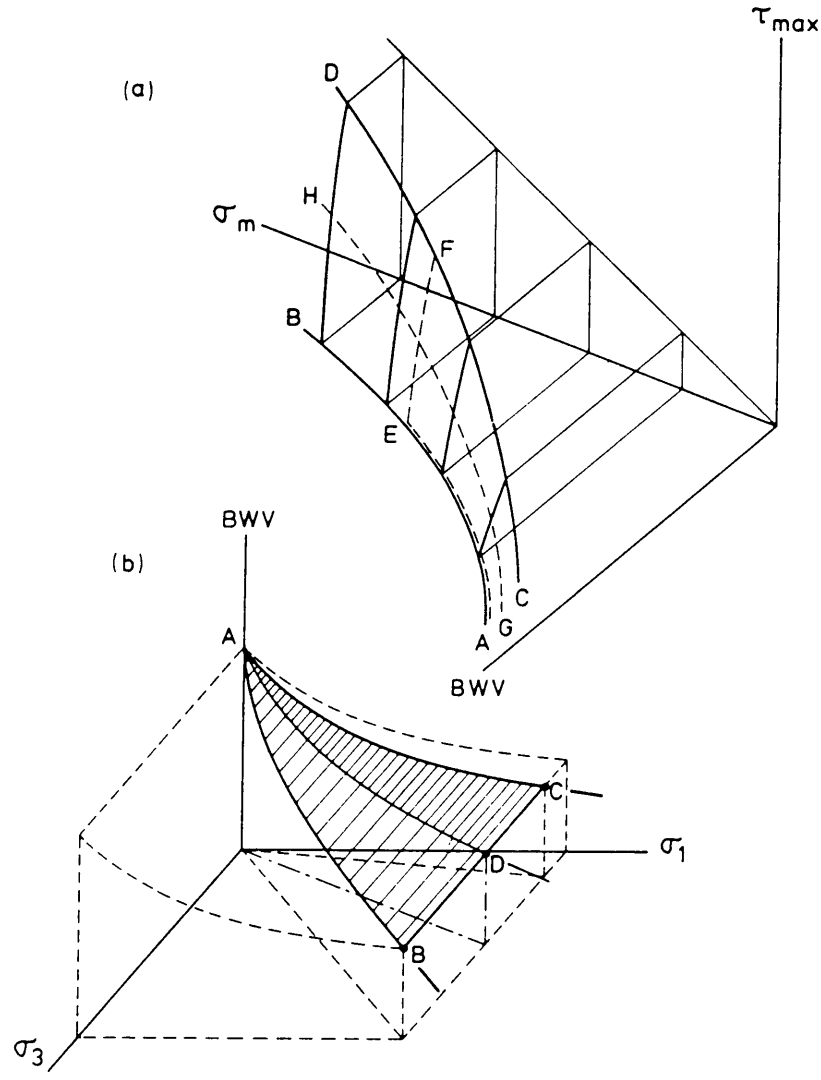


**Figure 1. Stress-strain and BWV relationship (Koolen and Kuipers, 1983)**

$$\left(\frac{\sigma_3}{\sigma_1}\right)_{cs} = \frac{3 - 2\left(\frac{\tau_{max}}{\sigma_m}\right)_{cs}}{3 + 4\left(\frac{\tau_{max}}{\sigma_m}\right)_{cs}}$$

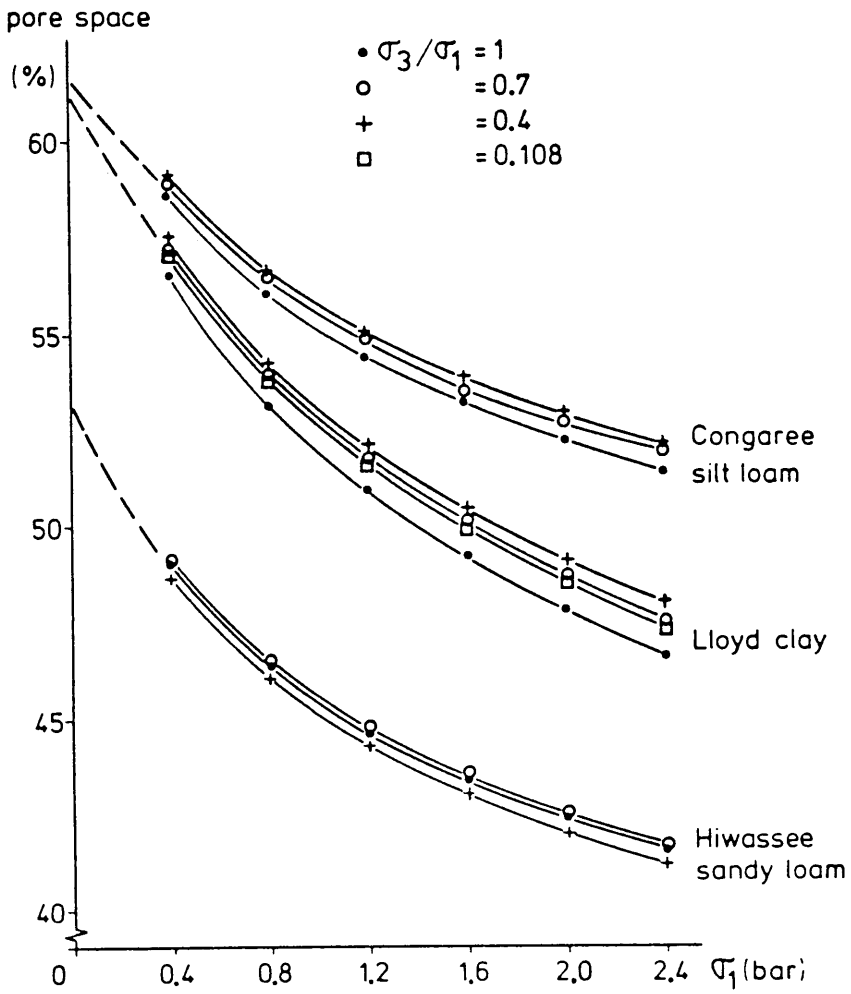


**Figure 2. Stress - pore space relationships (Koolen and Kuipers, 1983)**

velop compactibility models, and the soil uniaxially compressed follows curve AD (Figure 1) under loading at a constant diameter.

Bailey *et al.* (1984) developed a mathematical model for soil compaction. The model described satisfactorily the two extreme boundary conditions: if $\sigma_m$ equals zero then $\varepsilon_{v_s}$ also equals zero and as $\sigma_m$ goes to infinity the change in $\varepsilon_{v_s}$ becomes constant. The proposed equation is:

$$BWV = BWV_o - BWV_o \times (A + B \times \sigma_m) \times (1 - \exp[-c \times \sigma_m]) \qquad [10]$$

where,

$BWV_o$ = maximum bulk weight volume;

$\sigma_m$ = mean normal (hydrostatic) stress, and;

A, B, C = model parameters.

The model was evaluated using the triaxial test on Lloyd clay and Hiwassee sandy loam, and it was reported that the moisture content influenced all three model parameters (A, B, C).

Bolling (1985a) modified a triaxial apparatus to study the deformation of soil. Proportional load paths were applied on the soil samples at three principal stress ratios ($\frac{\sigma_1}{\sigma_3}$) of 1.43, 2.5, 3.3, and the deformations were recorded on a video camera. Curves of porosity to axial pressure were developed based on the experiments. The proposed section of the load compaction curve was approximated by the following relationship:

$$n = n_1 - \frac{[n_1 - 0.225]}{[35 \times c_p + 1]} \times \left[\frac{w}{12}\right]^{1.5} \times \sigma_{ax} \qquad [11]$$

where,

$\sigma_{ax}$ = axial pressure in kPa;

$c_p$ = ratio of radial to axial pressures;

n = % porosity;

$n_1$ = initial % porosity, and;

w = % moisture content (dry basis).

Bolling (1985b) studied the compaction of triaxial sandy loam soil samples. The compaction was related to varying moisture contents and initial bulk densities, and an equation was derived based on the measured bulk density response as:

$$n = n_1 - \left[\frac{w}{w_o}\right]^3 \times \sqrt{\frac{c_1}{c_{l_o}}} \qquad [12]$$

where,

$w_o$ = % initial moisture content (dry basis);

$c_1, c_{l_o}$ = current and initial core indices kPa;

$n_1$ = 57%;

$w_0$ = 8.36%, and;

$c_{l_o}$ = 100 kPa.

Grisso (1985) used a computer controlled triaxial test to apply deviatoric stresses on four different agricultural soils and observed the volume changes under two different load paths. The orthogonal, where the deviatoric stress was increased at constant mean normal stress, and the proportional, where the deviatoric stress was increased at constant confining pressure. It was concluded that for the same state of stress clay soils experienced greater volume change than sandy soils. At the same time, a small

difference in volume change for the same soil type, attributed to the load path, was observed.

Standard triaxial tests are generally conducted at very slow rates of loading (i.e. 1 to 3 mm/min). As a result the stresses, at any point in time, can be assumed equally distributed to all the points of the sample. This may not be true when the rate of loading becomes higher and reaches a limit of a *critical speed*, at which the compressive strength becomes maximum, between 2 and 4 m/sec, (Koolen and Kuipers, 1983). The action is not transmitted at once to all the parts of the soil sample, and the soil appears to be stronger than when loaded slower.

## 2.2 Loading Rate Effects

Lambe (1951) investigated the loading rate effects on the compressive strength of a cohesive soil. It was concluded that for several clays the maximum compressive strength was 1.4 to 2.6 times the strength attained under a 10 minute loading span. A plot of the testing conditions and results for Boston blue clay is presented in Figure 3.

Lambe (1959), measured the friction angle of sand at different loading rates and concluded that it is independent of the loading rate. The average observed increase in tan $\varphi$ was between 1% and 2%. He speculated, however, that the effect might be different when only pure shear is applied to the sand, or at confining pressures in excess of 100 psi.

Lambe and Whittman (1969) considered the loading rate effect on pure sand. It was concluded that if the loading time is decreased to 5 milli-seconds instead of the

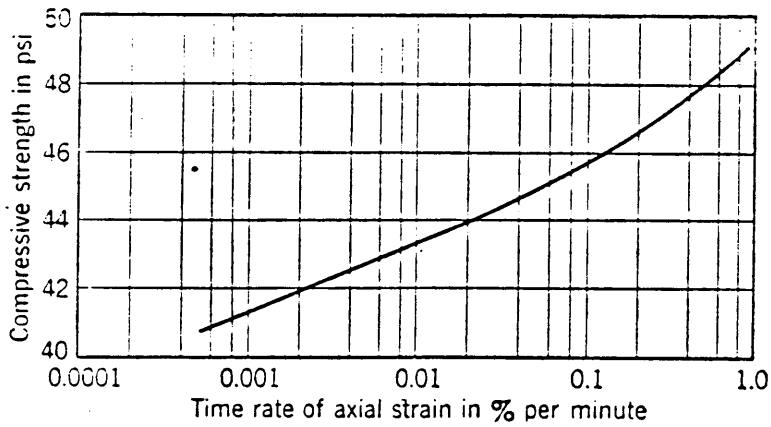


**Figure 3. Effect of loading rate on compressive strength on Boston Blue Clay (Lambe, 1951)**

standard duration of several seconds, the sample reacts as if it had double the usual compressive strength.

According to Lucius (1971) the compressive strength of the soil increases linearly with the logarithm of the loading ram velocity, up to a maximum and then decreases linearly with this loading ram velocity. An increase in compressive strength with increased moisture and clay contents was also observed.

Wu (1971), and Lucius (1971), measured the effect of the loading rate on the $\varphi$ and c parameters of the soil, and concluded that $\varphi$ is almost independent of the loading rate which means that c has to depend on it.

Rao and Hammerle (1973) conducted uniaxial tension tests on Hickory clay by varying the loading rates, temperatures and moisture contents, and concluded that the tensile strength of a sandy-clay soil appeared 1.3 times higher at 5 times higher elongation rate for all temperatures. They also reported that the samples appeared weaker with increased moisture levels.

## 2.3 Repeated Loading Effects

Seed and Chan (1961), considered the effect of duration of stress application on soil deformation under repeated loadings for sands and clays. It was concluded that the deformations experienced by both sands and clays are influenced by phenomena occurring during the intervals between the stress applications. For time intervals up to 2 min., silty sands experienced increased deformation with increased durations of stress application. On the other hand, silty clays experienced increased or decreased deformation, depending on the time interval and effects like creep,

anisotropy, stiffening due to repeated loading, and separation of clay particles during the unloading periods.

Lambe and Whittman (1969), investigated the effect of repeated loading for sand and clay samples. It was established that repeated loadings of the sandy samples will cause a change in $\varphi$ independently of the time interval between the loadings. More specifically, loose sand will densify resulting in strength increase and dense sand will expand resulting in strength decrease. Also, stress applied repeatedly can cause very large strains provided that the stress level is less than the maximum static stress at failure. The secant modulus, defined as the slope of a straight line connecting two separate points on the stress-strain curve, was employed in order to define more accurately the inelastic behavior of clay samples. It was concluded that the secant modulus increases during successive loading cycles. This increase is greater during the first two loadings and decreases for subsequent loadings. Figure 4 presents the variation of the secant modulus under successive loading cycles.

Wu (1971), concluded that fatigue failures similar to the ones occurring on steel and concrete may occur in soils due to repeated loading cycles.

## 2.4 Volume Change Measurements

In partially saturated samples volume changes occur due to changes in axial load or cell pressure. These changes may vary from 10% to 25% depending on how compacted or loose the soil is. The volume change measurements are important in order to determine the compactibility of the soil and to derive constitutive relationships.

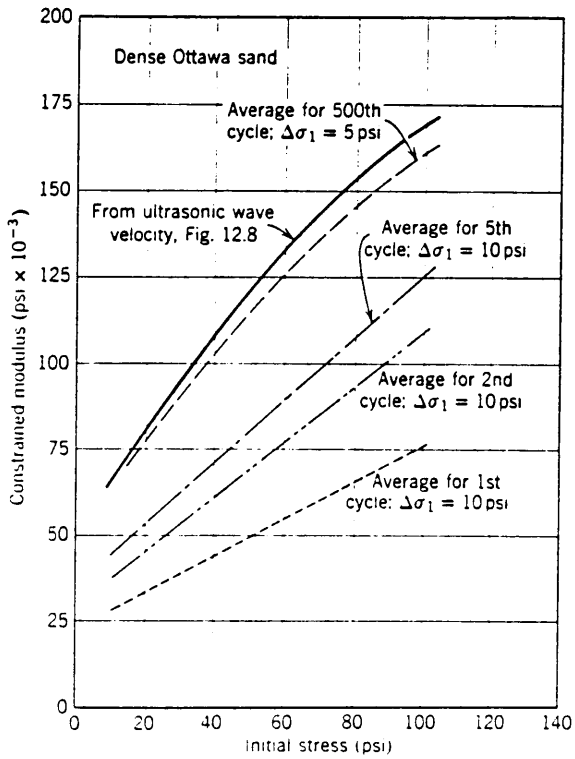


**Figure 4. Secant modulus with successive loading cycles (Lambe and Whittman, 1969).**

Bishop and Henkel (1957), presented two methods for recording the volume changes during a triaxial test.

- The self-compensating mercury manometer in which the displacement of the surface between the water and mercury is observed. The movement of the mercury is proportional to the water entering or exiting the cell, thus proportional to the volume changes. To convert the measured displacement of water into an actual volume change in the sample, one must correct for the volume of water displaced by the loading ram.
- The direct strain measurement method which can be used for the following cases:
  - When the soil is isotropic and volume changes can be obtained directly from axial strain measurements.
  - Under conditions of zero lateral strain, (earth pressure at rest), where there is no shear at the surfaces of the sample in contact with the end caps and the cross-section is maintained constant. In this case, the axial load must be increased slowly and the cell must be adjusted for zero lateral yield.

Hovanesian and Buchele, (1959), developed a volumeter based on the measurement of the air quantity forced out of the sample during compression. A diaphragm with strain gages was connected in line with the drainage valve of the loading pedestal. In that way the air forced out of the sample forced the membrane to deform. The results obtained were not very accurate since the heat transfer effects were not considered by the investigators.

Bishop and Donald (1961) developed a volumeter that uses paraffin or kerosene as the second liquid to interface with the water displaced by the soil sample. A gradu-

ated glass tube is filled up to one third of its height with paraffin and then is connected with the triaxial cell. At the same time the other side of the tube is connected to the pressure control line. The principal of operation is similar to the self-compensating mercury manometer but in this case no pressure compensation is necessary since the specific gravity of the paraffin or the kerosene is very close to the one of the water. In addition the system is safer to operate since the danger of mercury is eliminated, and it is cheaper to operate.

Dunlap and Weber (1971) modified the volumeter introduced by Havanesian and Buchele (1959) by submerging it in a water bath. The water surrounding the soil sample and the volumeter was at room temperature, thus the process could be assumed a constant temperature one. The relationship between pressure and volume in the test before and after the stress was applied was: $P_1V_1 = P_2V_2$, where, $P_1, V_1$ are the initial pressure and temperature and $P_2, V_2$ are the final ones. The same technique was used by Grisso (1985).

# Chapter 3

## *Experimental Procedure*

The triaxial apparatus is the most widely used and most versatile means of observing the shear strain characteristics of soils. A cylindrical soil sample is enclosed in a pressurized chamber which subjects the sample to compressive stresses in three mutually perpendicular directions.

### 3.1 Test Facility

#### *Triaxial Cell*

A conventional triaxial cell was used during this study. The cell jacket was constructed of clear plexiglass, 1.9 cm thick, and the aluminum top and bottom platens were 22.9 cm in diameter and 2.54 cm thick. The cell assembly was held together with six aluminum rods 1.9 cm in diameter. The pedestals were 7.1 cm in diameter. A 2.54 cm rod, which passed through the center of the top plate of the triaxial cell with the pedestal, was used to load the sample. One O-ring at the bottom plate, between the jacket and the cell base, and two around the rod on the top plate kept the fluid in the cell from leaking. The cell had two valves on the bottom plate to fill the

chamber with water and to apply the confining pressure. Two additional valves were available on the bottom plate for draining the soil sample, but they were not utilized during these experiments. The two valves available on the top plate were utilized to let the air out of the chamber when it was filled with water and to locate a pressure transducer to monitor the confining pressure. Figure 5 shows a photograph of the triaxial cell used in the experiments.

### *Volume Measurement*

The procedure used for volume measurements is a modification of the method developed by Bishop and Henkel (1957) (Figure 6). The basic idea of this method is to record the volume of water entering or exiting the cell and was discussed in the literature review. The drawback of this technique is that volume measurements correspond to very slow rates of testing. The readings were taken manually since they corresponded to static conditions. For the purpose of these experiments, readings under dynamic conditions were necessary in order to observe the compaction during loading at rates approximately 200 times higher than standard loading rates.

A cell compensating manometer was constructed for this purpose. The manometer was made of a 41 cm long transparent cylinder 2.54 cm in diameter. The top end of this cylinder was connected to one of the bottom plate valves of the triaxial cell via a .20 cm flexible tubing. The bottom end of the cylinder was connected to a 34.5 kPa (5 psi) pressure differential transducer and to a fluid reservoir with the use of a T-shaped connection and .20 cm flexible tubing. The fluid reservoir was being supported by a spring in order to compensate for volume changes and at the same time keep the confining pressure constant. The top side of the reservoir was connected to a water tank and the air pressure line. The air pressure was regulated via a

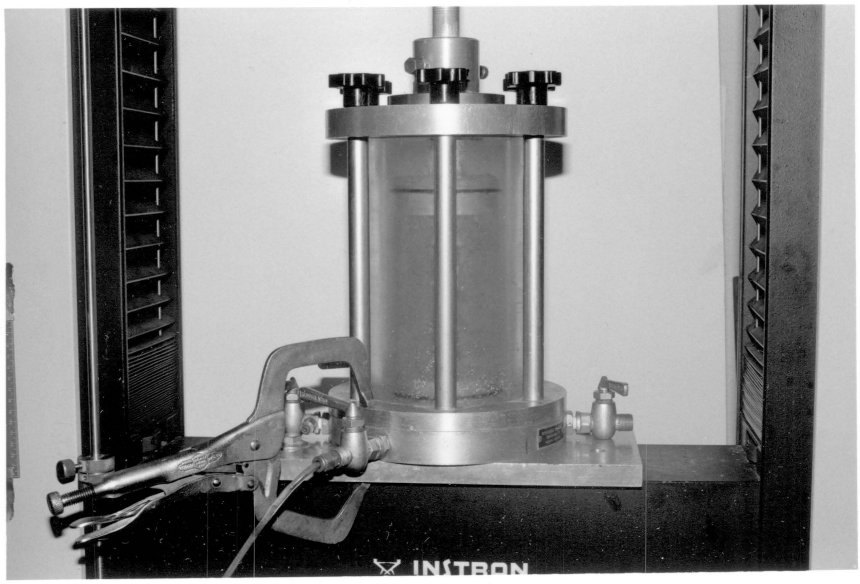


Figure 5. The triaxial cell

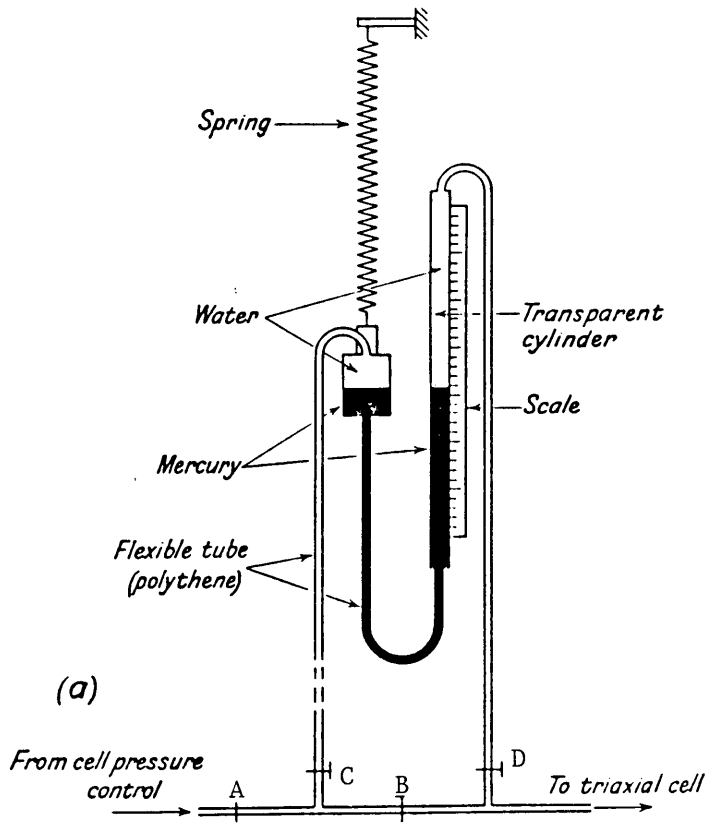


Figure 6. Apparatus for measuring volume change under pressure (Bishop and Henkel, 1957)

pressure regulator and a Bourdon gage with divisions 0 to 103 kPa (0 to 15 psi) in steps of 3.4 kPa (0.5 psi). When filling the cell with water, valves A, C, D, and B were closed. When the cell was completely filled with water, valves C and D were opened. At the same time the air pressure was raised and subsequently the appropriate confining pressure was applied to the sample, by opening valve A. Valve B was used to force any entrapped air out of the system before the test was initiated. This was accomplished by opening the de-aerating valve at the top of the cell while the system was pressurized and valves C and D were closed. During the test valve B was also kept closed.

The cylinder was filled with mercury up to one-third of its height making the interface between water and mercury clearly visible and a pressure reading obtainable. A change in volume of the soil sample would cause a head change in the interface, resulting in a change on the transducer's indication. Figure 7 shows a photograph of the modified volumeter used in the experiments.

### *Loading Frame*

The soil sample was axially loaded with the use of an Instron (Model 1123) testing machine. The Instron was equipped with 5 kN reversible load cell that was connected to the loading rod. The rate, direction of loading and the maximum applied load could be preset on the machine. The rates of loading could vary from 0.5 to 500 mm/min. The option of instantly unloading the sample after it had reached the maximum applied stress was available. Manual operation was also possible and used to place the sample onto the frame. A chart recorder with variable speed and direction of motion was used to determine when the loading rod came into contact with the soil.

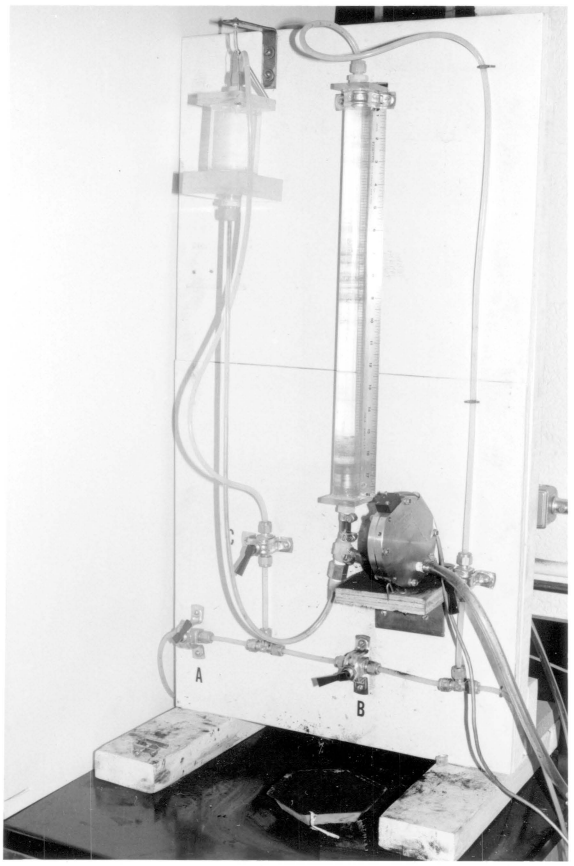


**Figure 7. The modified volumeter**

### *Instrumentation*

The items used for data collection were:

- An Apple II+ microcomputer.
- An Instron (Model 1123) loading frame equipped with a 5 kN force transducer mounted on the loading frame.
- A 12-bit Analog to Digital (A/D) converter.
- A Validyne differential pressure transducer, model DP103, equipped with a 0-5 psid membrane.
- A Celesco transducer indicator model CD25A.

The Apple II+ microcomputer was used to control the Instron and record the output from the load cell on the Instron loading frame and from the pressure transducer through the indicator. The microcomputer controlled the rate of movement of the loading frame and thus the loading rate of the sample, and the maximum load exerted on the sample. A program developed for this purpose monitored the axial force on the sample during loading and unloading. The inputs were maximum load force during loading, minimum force during unloading, rate and direction of loading. During the tests, the microcomputer recorded the data from the load cell and the pressure transducer via the A/D converter at a rate of 13 analog points per second per channel. Figure 8 shows the setup used for the experiments.

The data was initially saved on a diskette on the Apple II+ system. Later it was transferred to the Mainframe for data reduction, analysis and to obtain plots. A listing of the program used for the calculations is included in Appendix A. Figure 9 shows a simplified flowchart of the procedure followed during the experiments.

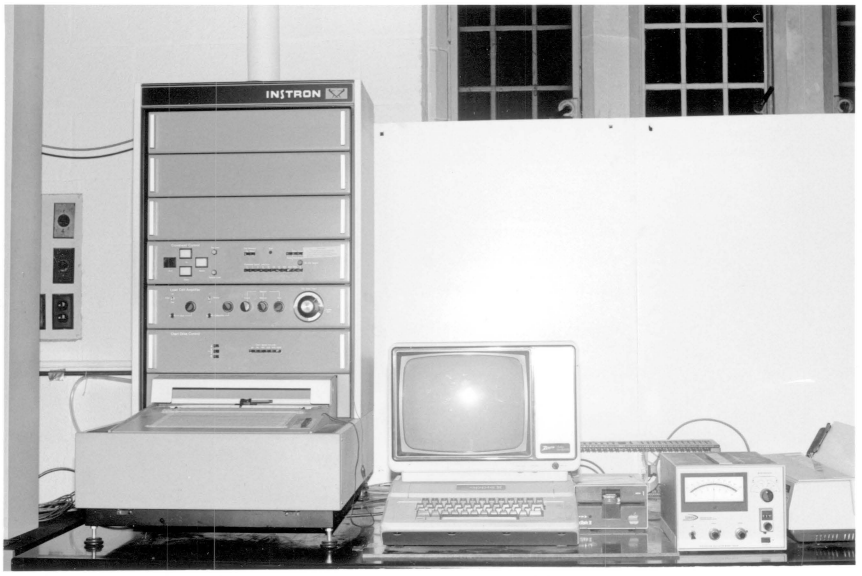


Figure 8. Test facility

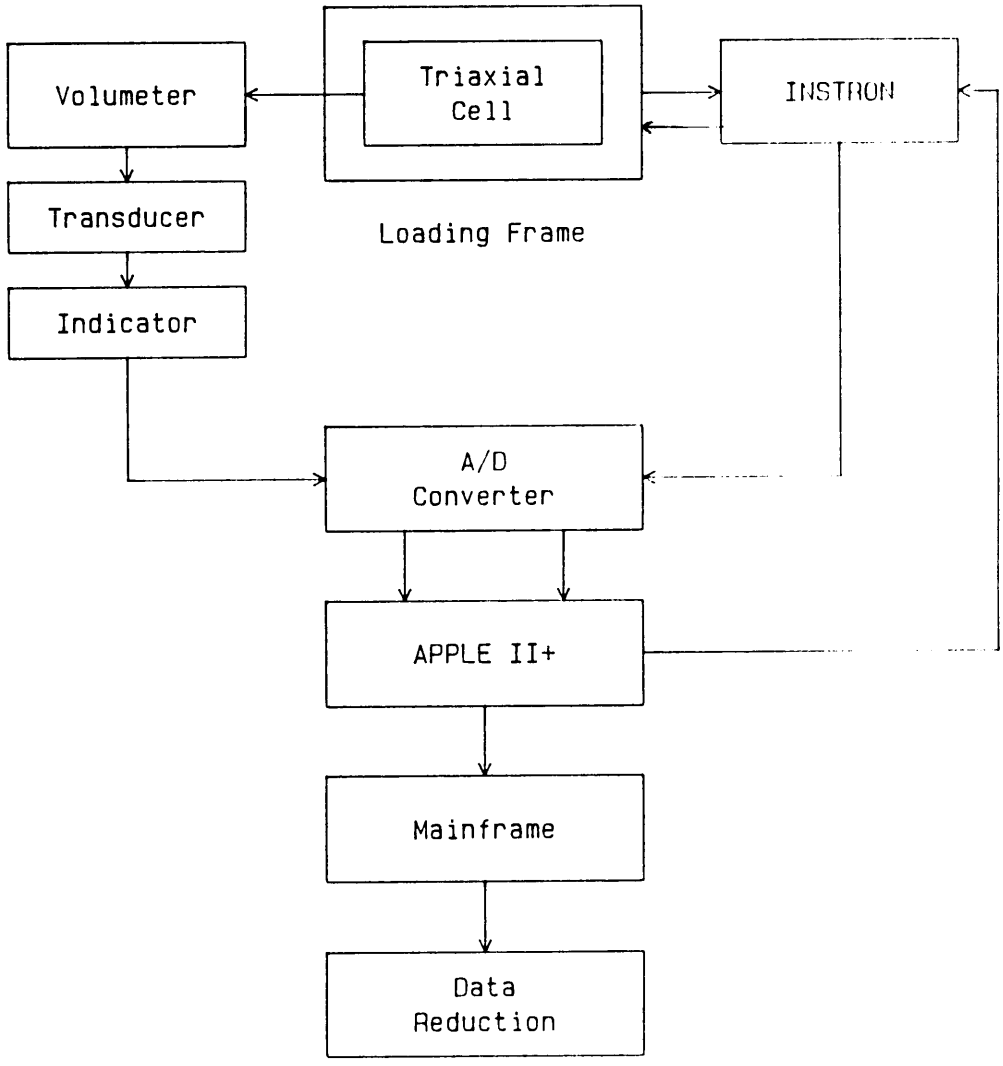


**Figure 9. Flowchart for testing soil samples**

## 3.2 Soil Used in This Study

The soil used in this study was the same as that used by Brandon (1987) and was supplied by Deere and Company. Based on results of grain size distribution analysis and Atterberg limits tests, Brandon (1987), classified the soil as sandy-clay. The grain size distribution data and results of Atterberg limits tests are shown in Figure 10 and Table 1.

Table 1. Atterberg limits, moisture level and density of soil samples.

| LL (%) | PL (%) | PI (%) | MC (%) | Density (g/cc) |
|---|---|---|---|---|
| 23 | 11 | 12 | 10 | 1.5 |

## 3.3 Sample Preparation and Testing

The soil was hand crushed into smaller particles using a mortar and a rubber pestle and sub-divided into quantities enough for a single sample before further processing. Then it was dried for 24 hours at 105° F. The following day the soil sample was raised to a moisture level of 10% and was placed in an air-tight plastic bag for a period of 24 hours for the moisture to reach equilibrium.

Initial tests were performed in order to obtain the frictional forces on the loading rod and to assure that the confining pressure was kept constant during the testing. Additionally calibration curves were obtained for the pressure transducer in order to convert the values of the indicator into volume change (ml) of the soil sample.

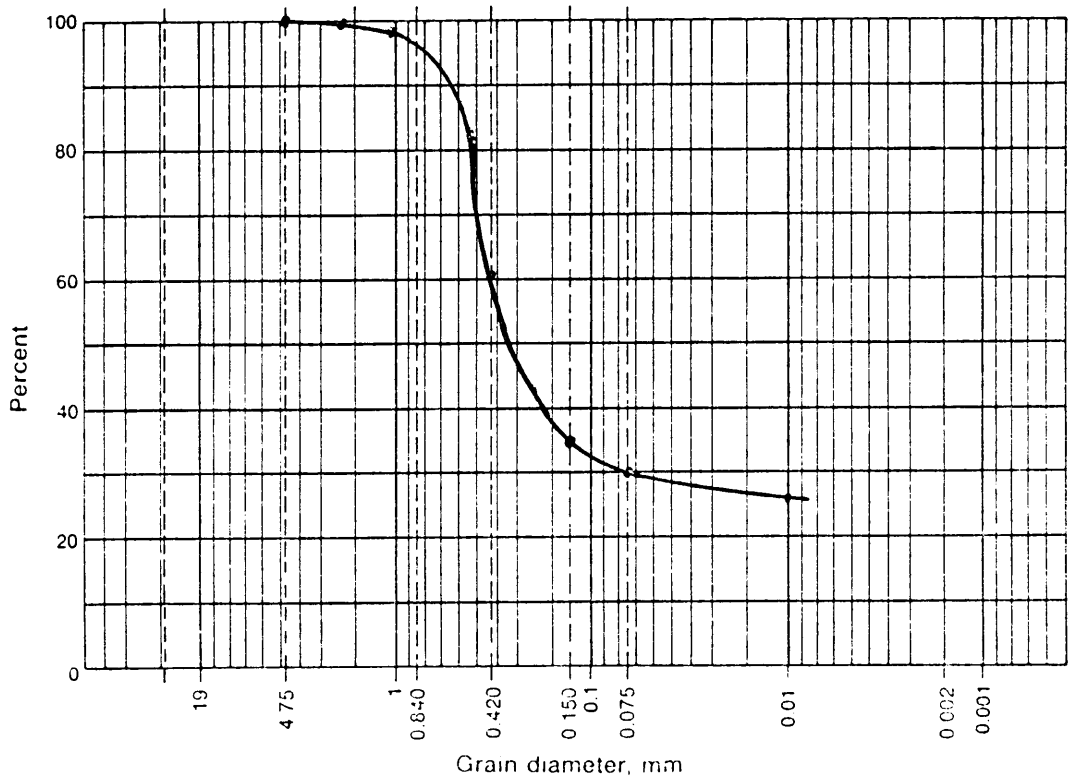


**Figure 10. Soil classification, (Brandon, 1987)**

To prepare the sample a rubber membrane was stretched around the bottom pedestal. A rubber O-ring was placed over the membrane to hold it against the pedestal. Silicon lubricant was placed around the O-ring and at the mating faces of the split mold to make it air-tight. Then the split mold was assembled ascertaining that the filter paper stripes (inside the split mold), were free of dirt and silicon. The upper end of the membrane was stretched over the top of the mold and subsequently a vacuum was applied between the membrane and the mold to hold the membrane against the mold walls. Figure 11 shows the equipment used towards preparing a sample.

The 7.1 X 15.24 cm cylindrical sample was prepared in twelve layers of soil compacted to the specified density. The weight of the soil for each layer was determined depending on the density. An electronic scale was used to accurately measure the weight of the soil per layer. Each layer was compacted using an aluminum piston and a rubber mallet in order to meet the specified compaction level (Ladd, 1978). After the soil was compacted into the mold it was assembled with the upper part of the triaxial cell and the loading rod which were already positioned on the Instron. The system was carefully aligned in order to avoid disturbing the sample and to keep the loading rod friction level constant between experiments. The tie rods were fastened and the cell jacket was filled with water. The desired confining pressure was applied by opening the bottom valve connected to the compressed air source. The system was left for approximately 15 minutes to reach equilibrium while the test conditions were entered in the data acquisition program controlling the experiment. Figure 12 shows the steps towards preparing and assembling of the triaxial cell.

Each sample was loaded and unloaded three times at a specified stress level for 10 seconds and then it was finally loaded at higher level for 5 seconds to achieve complete failure. It should be noted, that failure is assumed when the material reaches


**Figure 11. Equipment used towards preparing the samples**

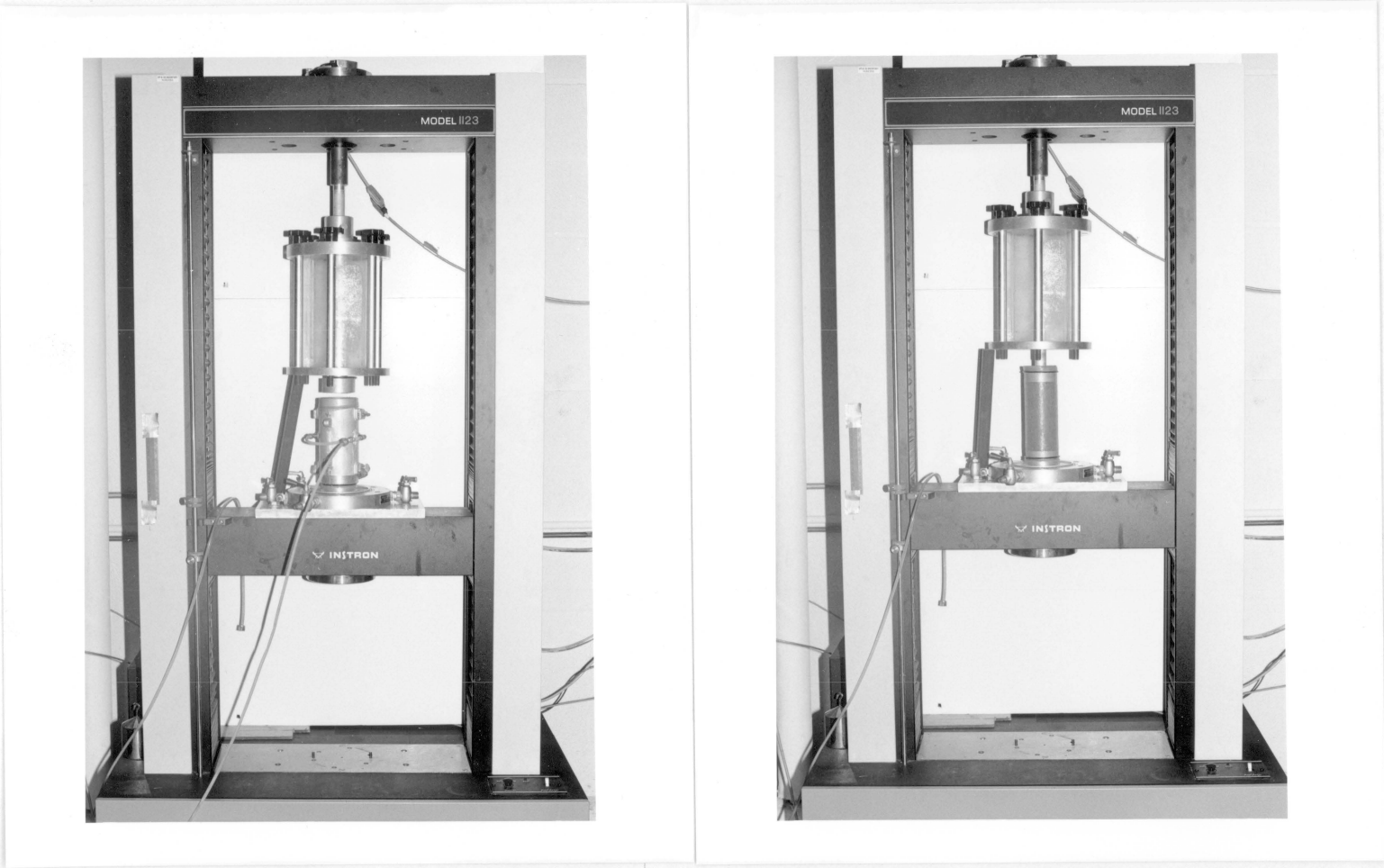


Figure 12. Triaxial cell assembly

its yield point, i.e. strain increases without any substantial stress increase. Tests were conducted under five different confining pressures of 13.8, 20.7, 27.6, 34.5 and 41.4 kPa (or 2, 3, 4, 5 and 6 psi respectively). The tests were replicated once at each confining pressure The maximum axial stress, for all tests, was 138 kPa for the first three loadings and unloadings and 170 kPa for the failure simulation.

# Chapter 4

## *Results and Discussion*

A volume measuring technique was developed and used to obtain stress-density data. In addition using the stress-strain relationships parameters for the elastoplastic model developed by Brandon were determined and the results are compared.

### *Verification of Volume Measurement Technique*

During initial testing, the electrical noise generated by various components with the system were picked-up by the transducer indicator and thus, subsequently, by the data acquisition system. Additionally, air entrapped between the mercury and the membrane of the transducer was responsible for inaccurate readings of the pressure head on the U-tube manometer. The first problem was eliminated by using shorter transmission lines for all electrical connections, making sure at the same time that the lines did not cross one another if it could be avoided. To overcome the second problem a VALIDYNE DP103 transducer was used that had the de-aerating valves next to the membrane. As an additional precaution, the mercury level was monitored at all times and in particular when the amount of water expelled from the cell was expected to be above average.

The system was tested at both high and slow rates to ascertain that volumetric changes are easily detectable by the apparatus used. For that purpose the cell was assembled and filled with water without including a soil sample. Then the loading rod was pushed into the cell at a predetermined rate. The amount of water expelled from the cell was easily calculated as a function of rod travel into the cell and rod diameter. The fact that the diameters of the rod and the inside dimater of the manometer tube were the same, simplified the calculations since the length of the rod advanced into the cell was equal to the vertical displacement of the mercury column. Preliminary tests to validate the volume measuring technique developed were conducted at three different rates of 5, 50 and 200 mm/min. At each speed the tests were replicated three times. The movement of the loading rod was controlled by the APPLE II+ microcomputer and checked with a ruler on the loading frame and on the U-tube. At the same time the APPLE recorded the values given by the transducer indicator. Figure 13 presents some of the data collected during the calibration procedure for a loading rate of 200 mm/min. When the loading rod moves for one second (equivalent to 13 sampled points by the monitoring program), the displaced volume of water was:

$$dV = \frac{200}{60} \times \frac{\pi}{4} \times (25.4)^2 \ [mm]^3 = 889 \ [mm]^3 \qquad [13]$$

The average of the digital readings for the pressure differential as calculated by the A/D conversion routine of the APPLE II+ was calculated equal to 511.2 units/second, which corresponds to 303 units/ml. Representative data for the calibration tests at different speeds are given in Appendix B.

The results were consistent for all rates of movement proving the ability of the system to record volume changes under high and slow rates of loading. The collected data

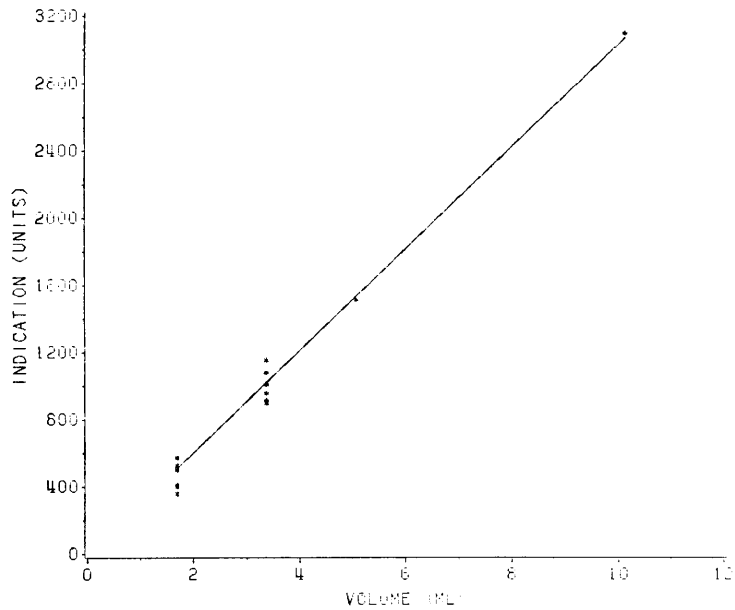


**Figure 13. Calibration curve for loading rate of 200mm/min.**

was used to develop a relationship between the indicated analog value and the actual volume change (in $cm^3$) that was subsequently utilized during data reduction.

### *Stress-Density Relationship*

Sample response was similar under the different testing conditions (i.e. confining pressure, axial load), thus, confirming the validity of the tests. The stress density plots (Figures 14 to 18) indicated a certain pattern in sample behavior during loading and unloading. During the first loading the density of the samples increased and upon unloading it decreased without returning to the initial value, thus indicating plastic deformation. Upon reloading, the density increased to a higher level than before, but when unloaded for the second time, it returned to the density level obtained at the end of the first load-unload cycle. Sample behavior during the third loading and unloading cycle was also the same. It was observed that during the two reloading cycles the density increased from the initial value up to almost the final value at low stress levels, and then it increased by a small amount even though the stress was increased to the limiting value. This response indicated that under a certain maximum load the soil density can be increased up to a certain value, which appears to be independent of the loading cycles for the specific initial density. During the final loading the sample's density increased since the sample was overcompacted to assure failure.

As the experiments progressed, dirt accumulated on the loading ram. Between the tests under 6 psi and the remaining sets of tests, the cell had to be removed from the loading frame a number of times to allow for different experiments to be performed. Upon re-assembly of the cell, alignment problems that occurred, led to excessive

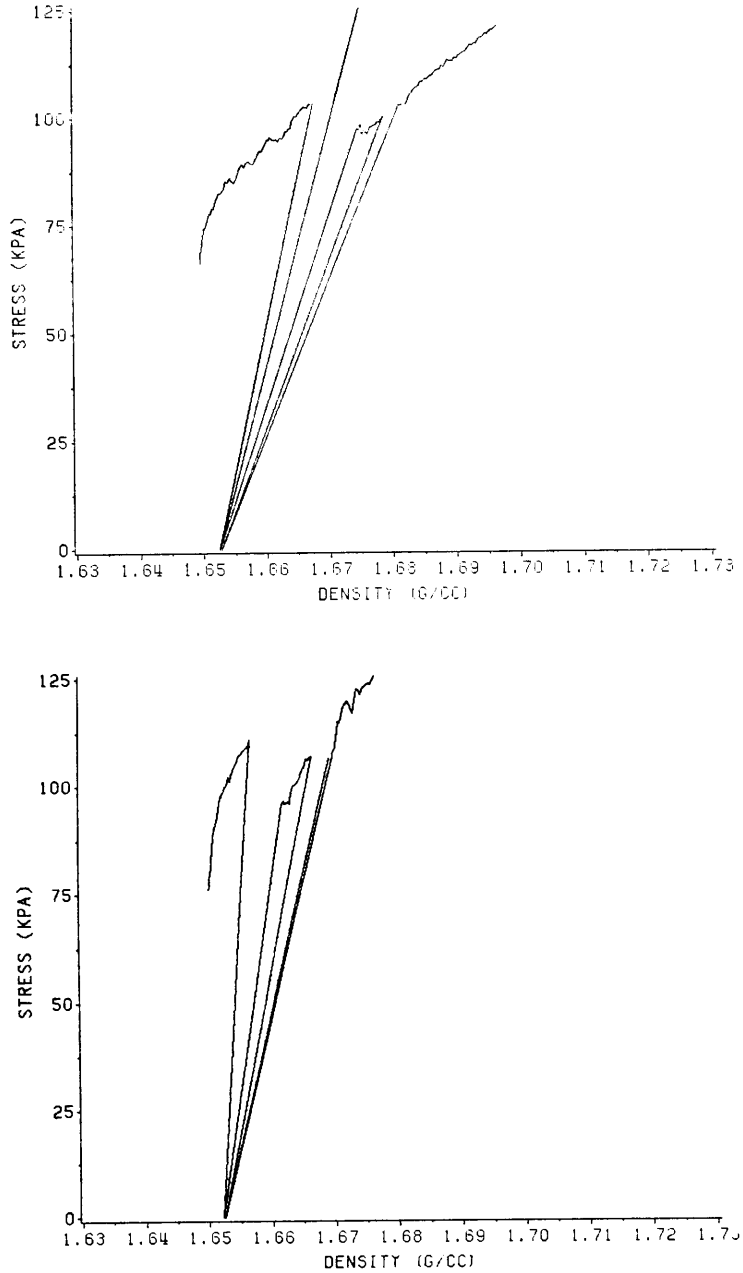


**Figure 14. Stress-density curves for confining pressure of 2 psi**

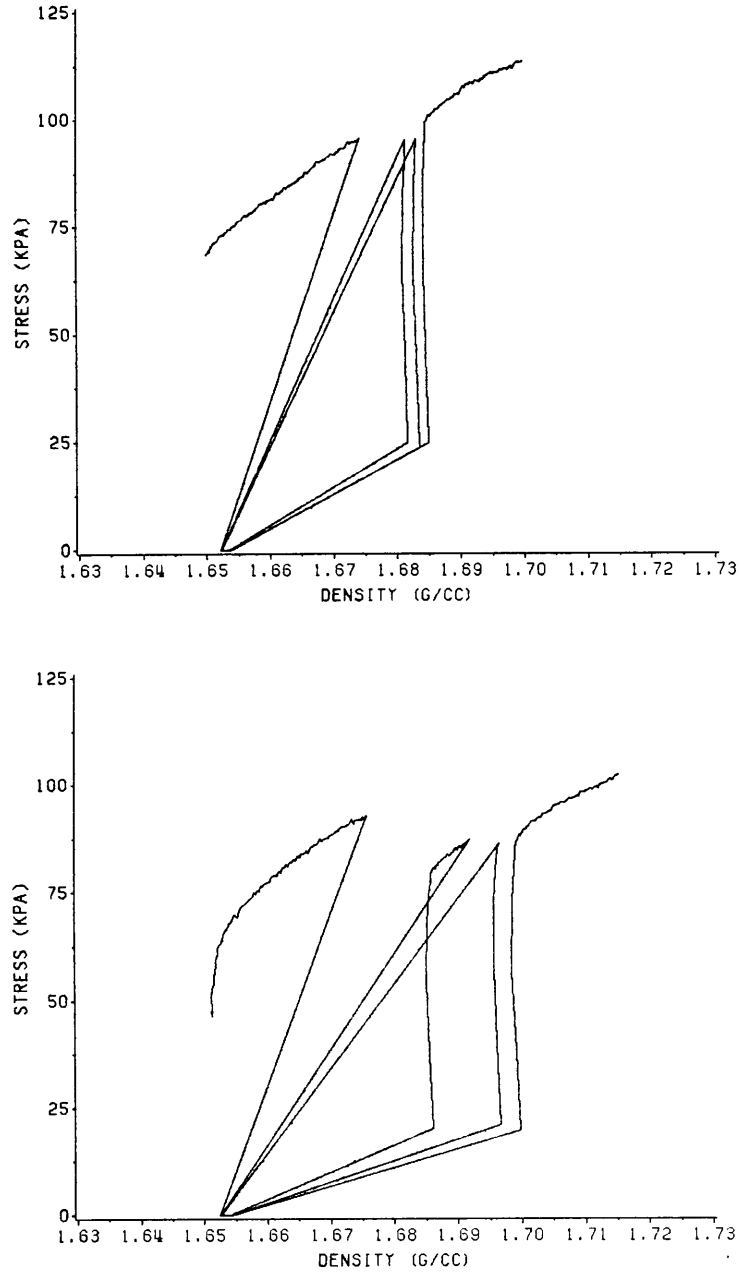


**Figure 15. Stress-density curves for confining pressure of 3 psi**

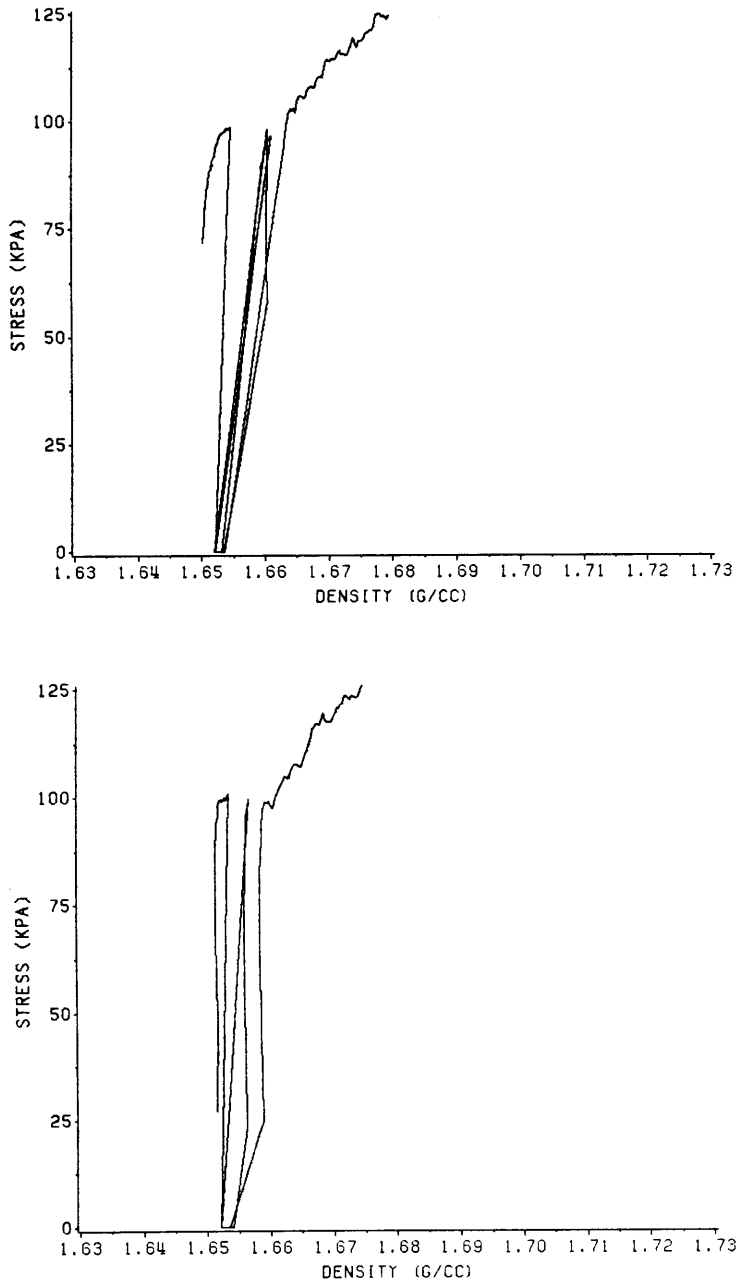


**Figure 16. Stress-density curves for confining pressure of 4 psi**

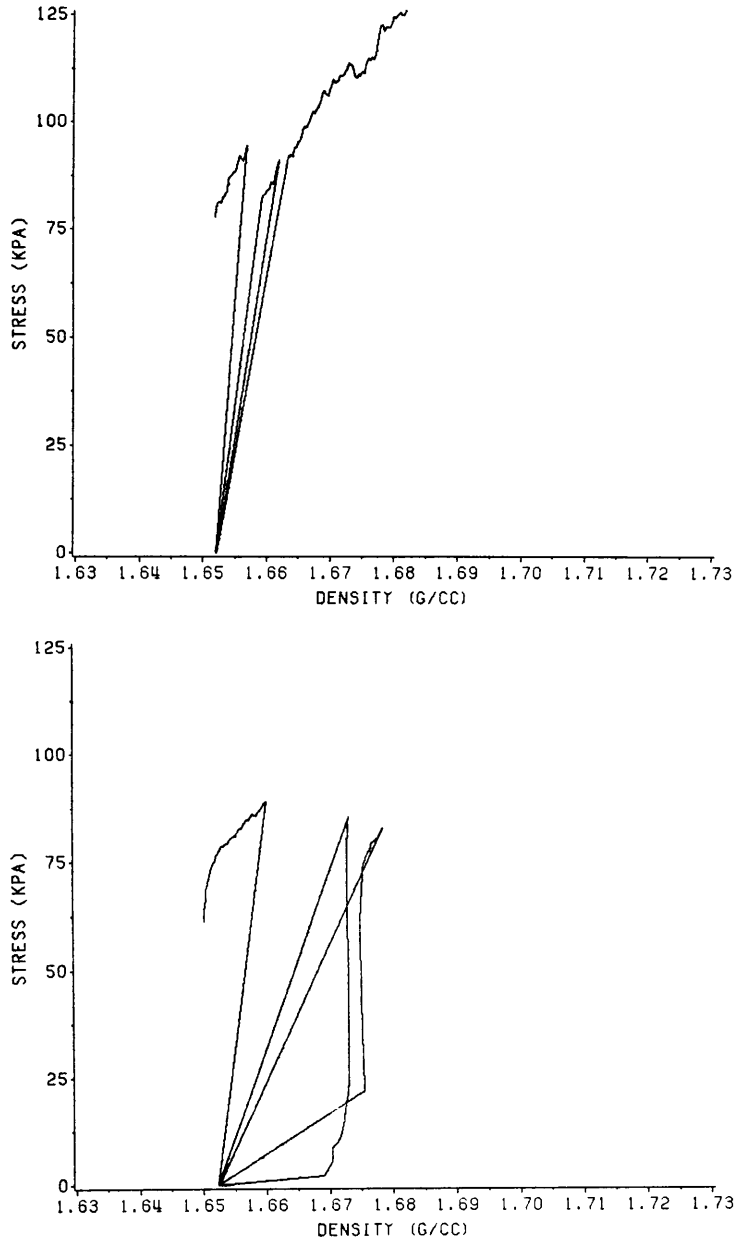


**Figure 17. Stress-density curves for confining pressure of 5 psi**

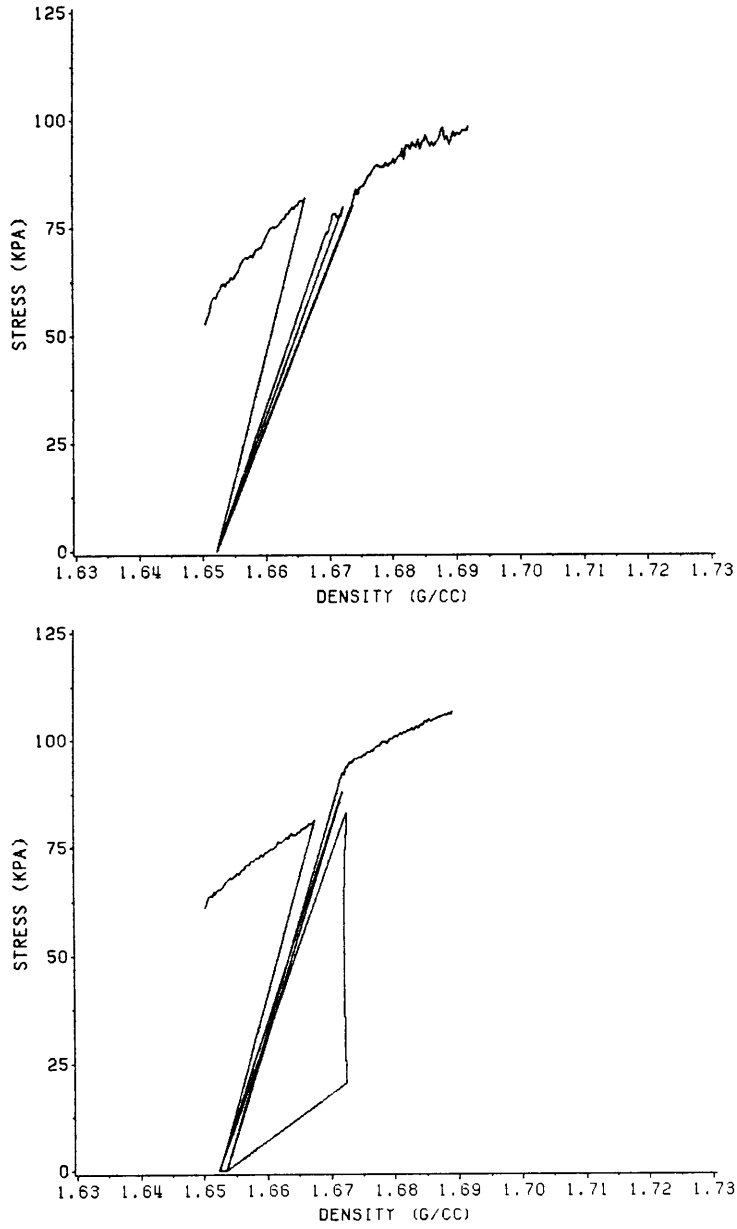


**Figure 18. Stress-density curves for confining pressure of 6 psi**

force readings and inconsistent replications. Additionally, it was impossible to do more replications for the unsuccessful experiments because the soil provided by Deere and Co was not enough.

Since the soil behavior followed a certain pattern, an attempt was made to develop a mathematical model for the first loading using the stress, strain and density data collected. The data was correlated using a General Linear Model procedure available in the Statistical Analysis System (SAS) to obtain regression parameters and the linear equation coefficients. Figure 19 shows the linear model obtained with a coefficient of determination ($R^2 = 0.70$). However, more experiments are needed over a larger range of confining pressures and initial soil densities before a generalized model for dynamic behavior of soils can be described.

### *Elasto-Plastic Parameters for the Soil used*

In order to determine the effect of initial density on the soil parameters, the Mohr-Coulomb failure criteria was used, which employs the following yield function for the plastic behavior of the soil:

$$f(\sigma) = c + ap - q = 0 \qquad [14]$$

where,

$p = \frac{(\sigma_1 + \sigma_3)}{2}$;

$q = \frac{(\sigma_1 - \sigma_3)}{2}$;

$c$ = the cohesion (intercept of the p-q line);

$a$ = the slope of the p-q line ($= \sin \varphi$).

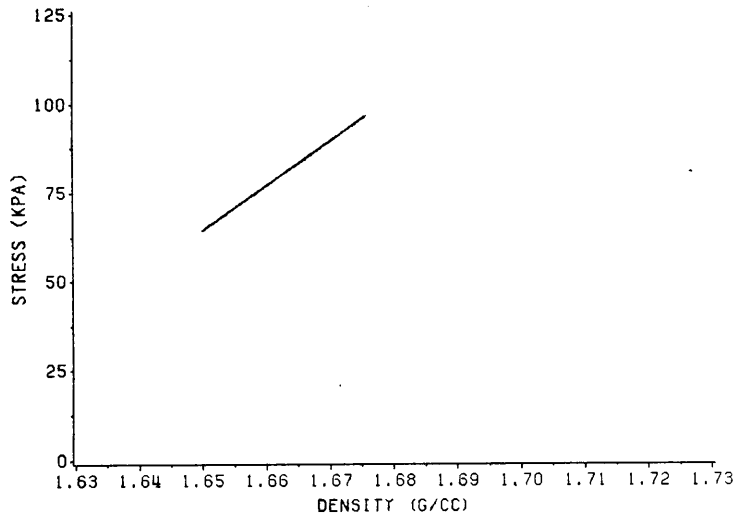


**Figure 19. Stress versus density (average curve for first loadings)**

In order to evaluate the soil parameters in the model, the maximum deviatoric stress levels (stress at failure) were obtained from the stress-strain plots (Figures 20 to 24).

Stress at failure was depicted as stress at yielding. Results for the different confining pressures were plotted on the p-q space and parameters a, c were evaluated. At the same time the average slope of the stress-strain curves (for the first loading) was used to calculate the modulus of elasticity, E. The value of the Poisson's ratio ($\nu$) was subsequently calculated based on the following equation:

$$\nu = 0.5 - \left[\frac{E}{6\,E_b}\right] \qquad [15]$$

where,

$E$ = modulus of elasticity;

$E_b = \frac{\sigma_1 + 2\sigma_3}{\varepsilon_v}$;

$\varepsilon_v = \frac{\Delta V}{V}$ = volumetric strain at failure;

$\sigma_1$ = principal stress at failure;

$\sigma_3$ = confining stress.

The calculated soil parameters are summarized in Table 2 along with the respective parameters calculated by Brandon (1987). Figure 25 presents a comparison between results obtained by Brandon and results obtained during this study for a confining pressure of 6 psi.

It can be concluded from the results presented above that the increase in the initial density (from 1.50 to 1.65 g/cc) affect the calculated soil parameters. In a comparison with the results obtained by Brandon (1987), as expected the soil is stiffer since its modulus of elasticity was calculated 59% higher than before. Additionally, the soil

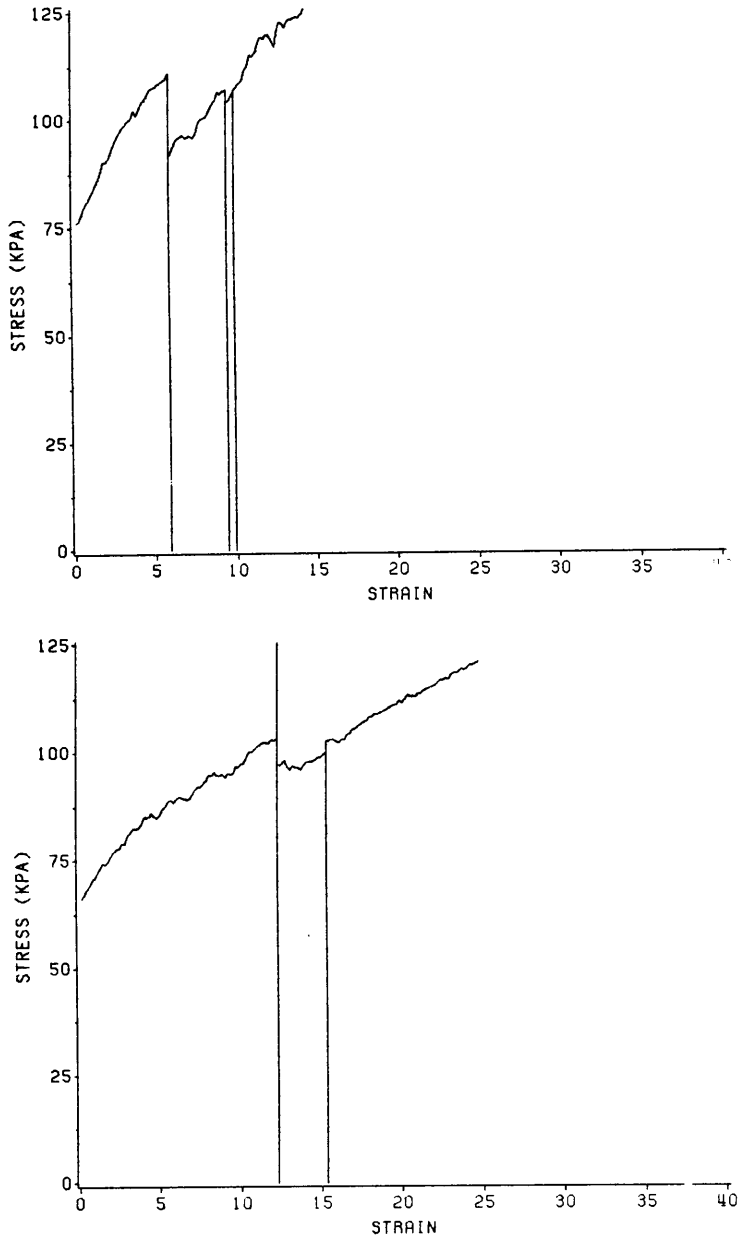


**Figure 20. Stress-strain curves for confining pressure of 2 psi**

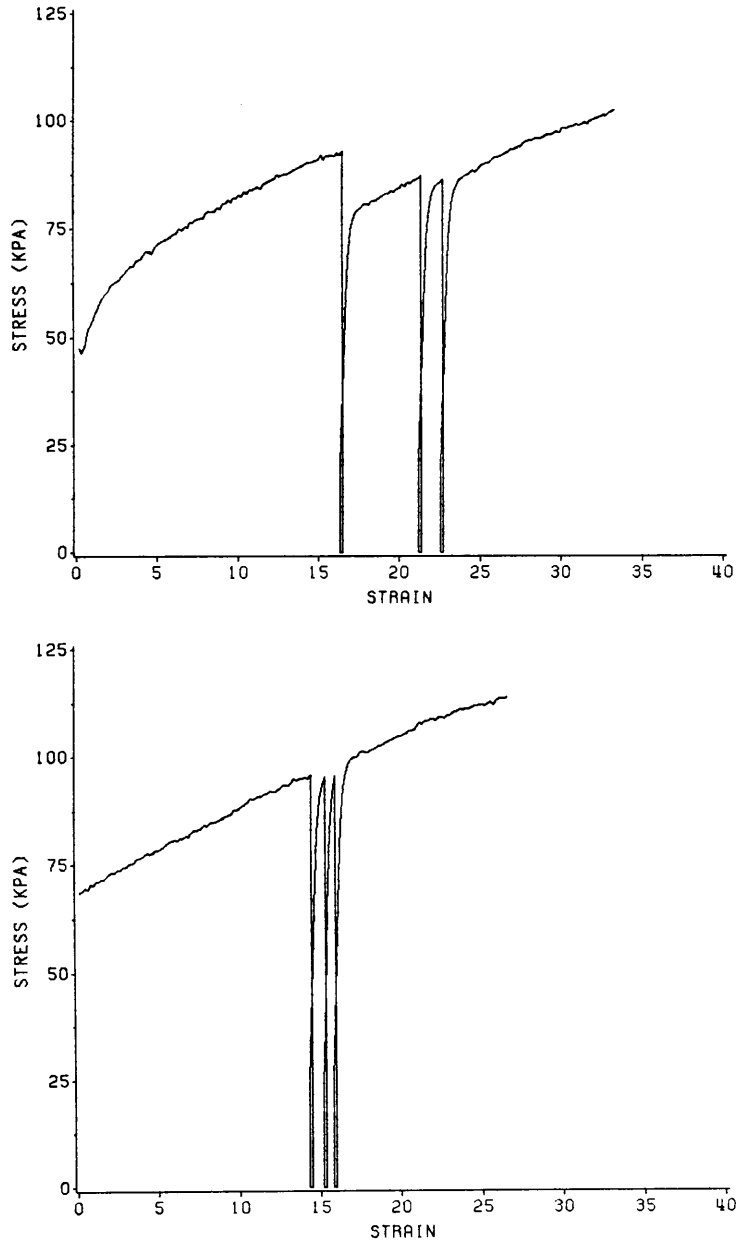


**Figure 21. Stress-strain curves for confining pressure of 3 psi**

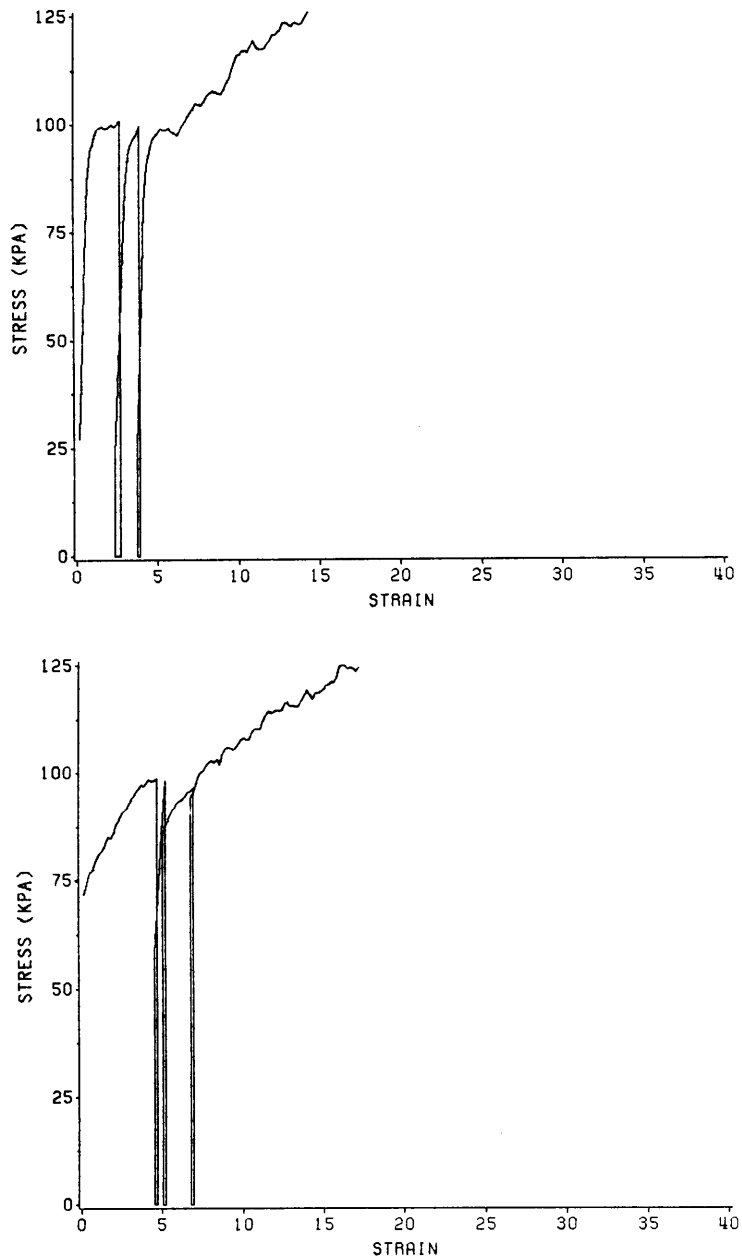


**Figure 22. Stress-strain curves for confining pressure of 4 psi**

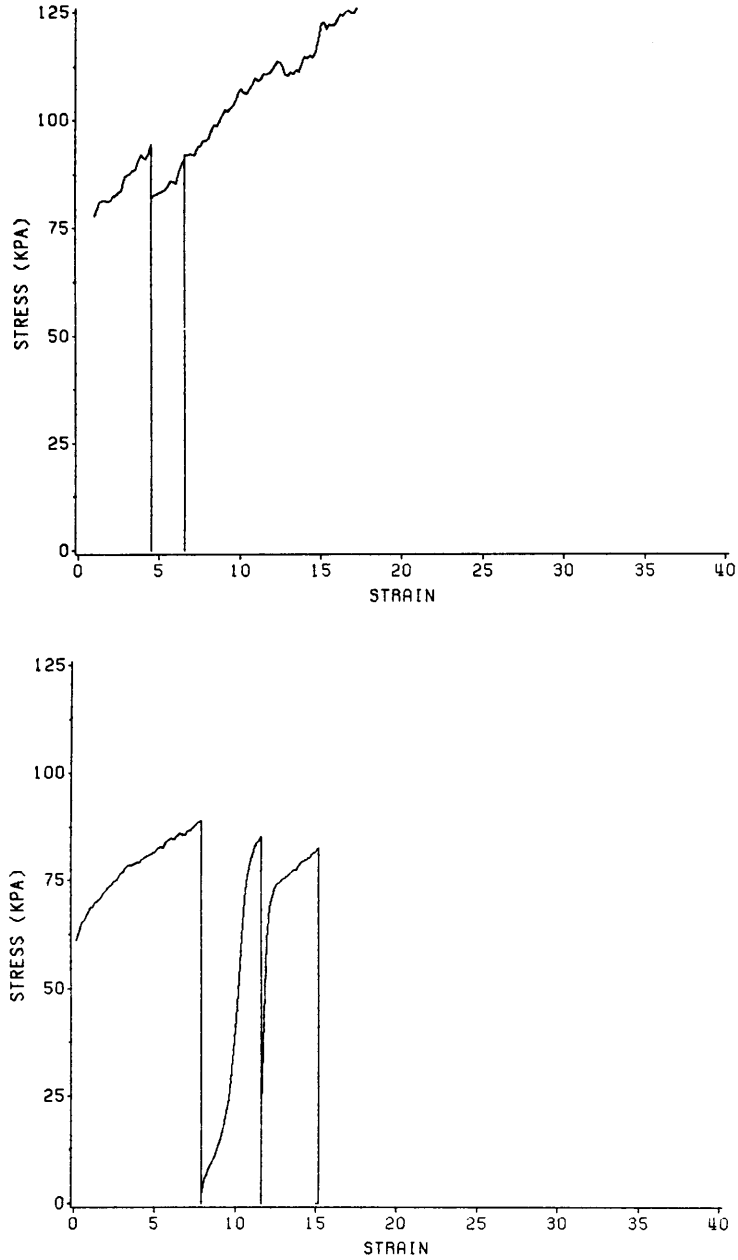


**Figure 23. Stress-strain curves for confining pressure of 5 psi**

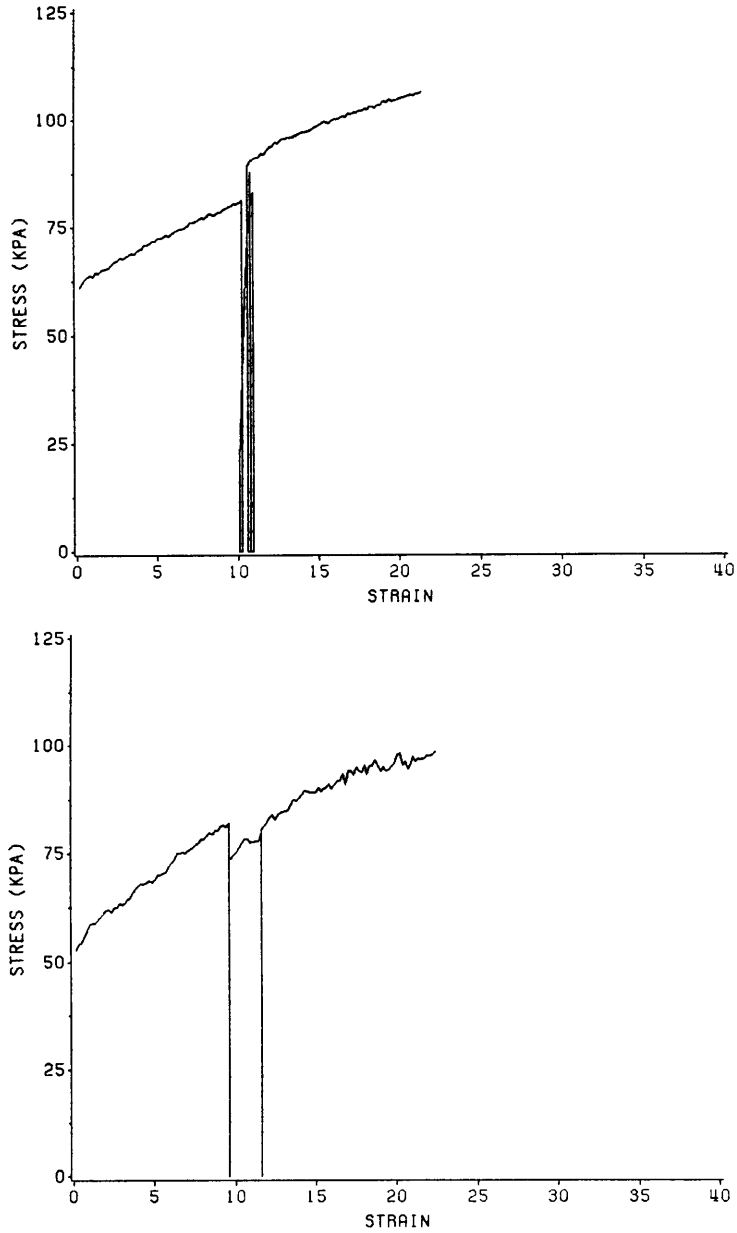


**Figure 24. Stress-strain curves for confining pressure of 6 psi**

Table 2. Comparison of the Parameters Calculated by Brandon (1987) to these obtained in this study.

| | This study | Brandon (1987) |
|---|---|---|
| Failure Criterion | Mohr Coulomb | Mohr Coulomb |
| Initial Density | 1.65 g/cc | 1.5 g/cc |
| E | 170 MPa | 107 Mpa |
| $\nu$ | 0.25 | 0.42 |
| $\varphi$ | 14 | 12 |
| c | 24 kPa | 32 kPa |
| a | 0.25 | 0.21 |

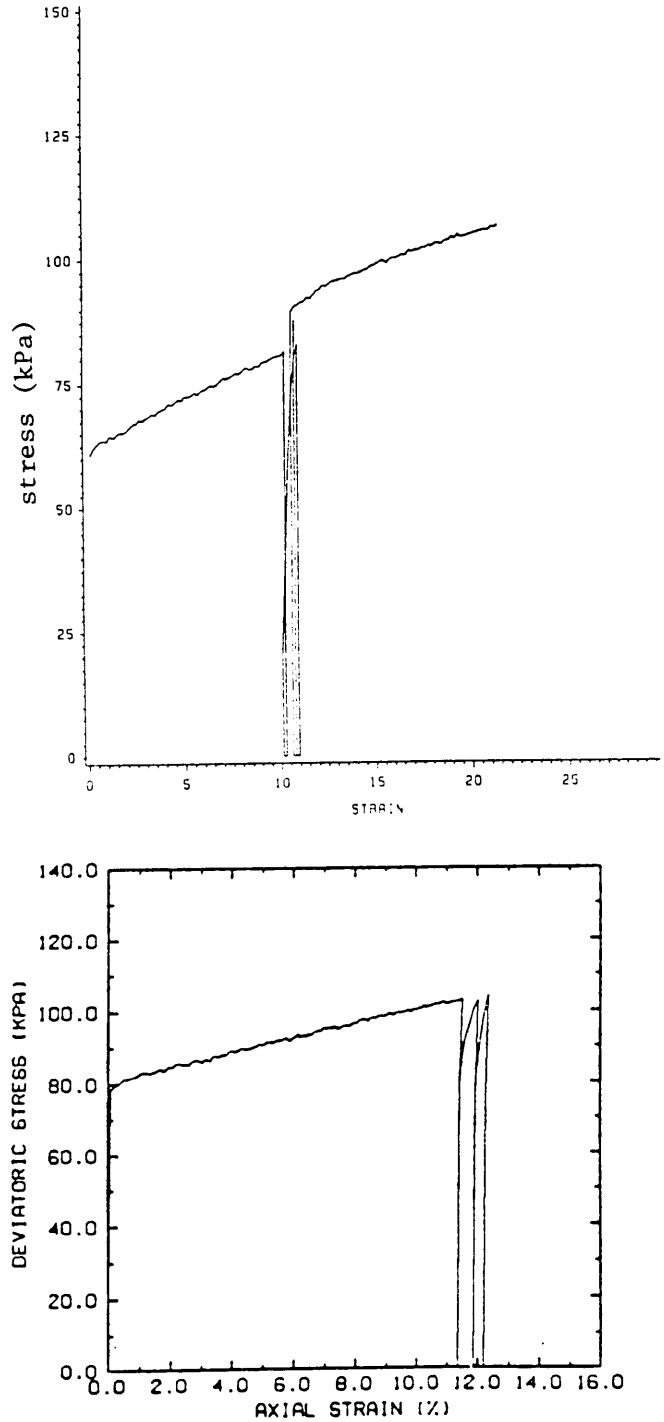


**Figure 25. Comparison of stress-strain curves for confining pressure of 6 psi**

cohesion (c) was 28% less, while the angle of internal friction (phi.) was 17% more for the samples tested in this study. It should be noted that the particle size that comprise each sample is known to affect the cohesive properties of the soil. For the same clay contents of the soil, the finer the soil particles are, the greater the specific surface, and, thus for the same moisture content, the higher the interaction forces between clay particles. Therefore, differences in the cohesive properties of the soil can be attributed to differences during preparation of the samples, since soil grinding was performed manually. As already mentioned, the experimental results were used to obtain the volumetric strain at failure and subsequently calculate the average value for the Poisson's ratio. This value, however, cannot be compared to the one reported by Brandon (1987), since he assumed a value for the Poisson's ratio due to the lack of volumetric strain data. Further differences between the results can be attributed to the fact that, in this study, the time interval between initial loading and failure of every sample was considerably reduced, due to the data acquisition software, which was enhanced to allow for both compression and tension monitoring under the same computer program. Thus stress re-distribution within a sample was minimized, as is the case in actual dynamic loading conditions. Finally, the arbitrary definition of the failure point on the stress-strain curves contributes to differences observed for replicating tests in this study as well as those reported by Brandon (1987).

The discrepancies on the replicated tests may be attributed to the conditions explained below:

A serious problem was that the alignment between the loading rod and the triaxial test fixture caused increased friction between the rod and the entry on the cell resulting in lower values of maximum load. Additionally, rotation of the sealing O-rings could cause variation in the friction on the loading rod. Although the samples were

prepared very carefully, the non-uniformity in the soil grains and the disturbance on the sample when positioned in the triaxial cell allowed for different compaction characteristics under similar loading conditions. Furthermore, the confining pressure supply valve had a wide range of adjustments resulting in different pressure settings for replicating experiments. Finally, the experiment was conducted in water which could not be fully de-aerated and air bubbles were always present on the cell walls.

Further studies should be conducted under different testing conditions (i.e. initial density, range of confining pressures, loading rates, etc), to fully describe the soil behavior under dynamic loading. Additionally, it should be noted that the strain-density curves developed in this study (Figure 26) strongly suggest that a relation-ship could be established between strain and density.

### *Suggestions*

The following suggestions can be made in order to improve the testing procedure and reduce the variation in the results. Consistent particle distribution should be main-tained to minimize differences due to cohesion forces. An amphibious transducer (i.e a transducer capable of operating under water), would eliminate the problem created by the friction on the loading rod since force reading could be obtained directly from the loading pedestal. Additionally, the bottom platen of the triaxial cell can be placed on rollers to allow the system to self-align during installation of the cell. For even higher loading rates, a damping device might be necessary to compensate for inertia problems together with the already existing spring supporting the mercury tank. Finally, a different type of triaxial cell that could be easily assembled would eliminate the sample disturbance problems occurring during sample positining in the cell.

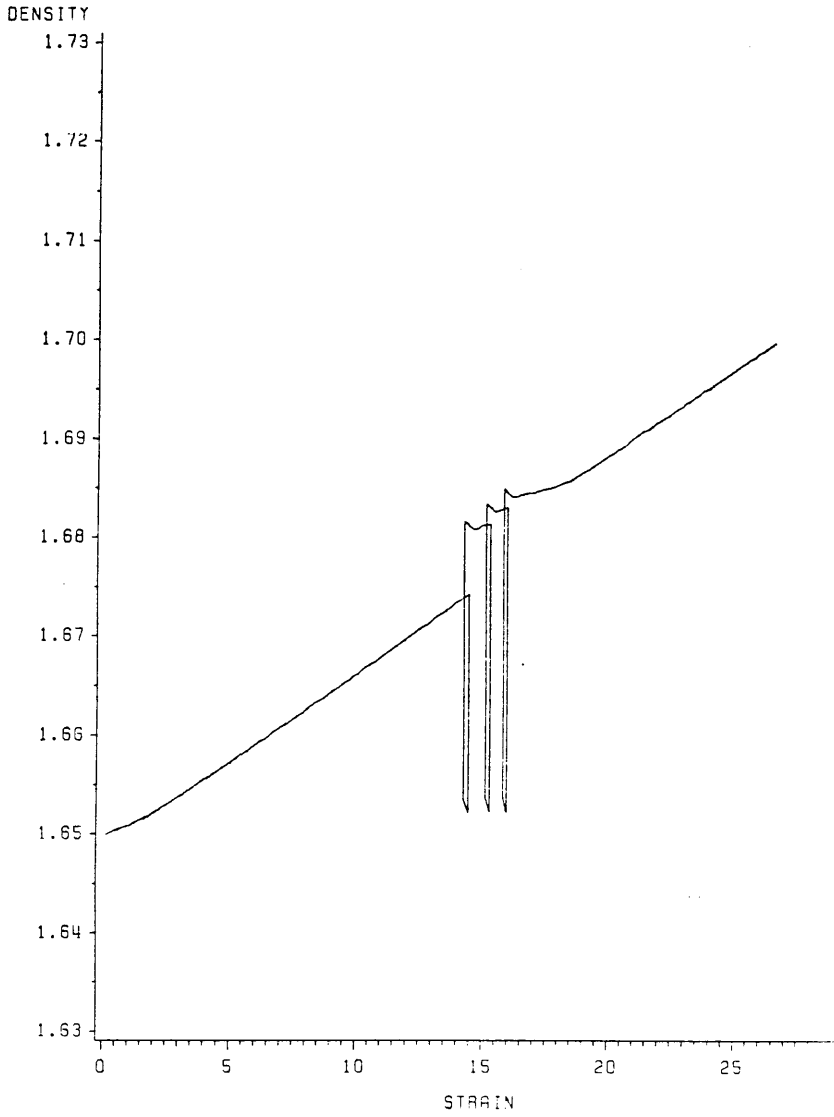


**Figure 26. Density-strain curves for confining pressure of 3 psi**

# Chapter 5

## *Summary and Conclusions*

A stress-density model for agricultural soils was developed in this study by measuring soil responses under dynamic loading. A volume measuring technique was developed to record the volume changes of the soil samples at high loading rates. The volumeter introduced by Bishop and Henkel (1957), was modified by adding a pressure transducer capable of recording the pressure head changes under simulated dynamic conditions. The ability of the system to respond to the testing conditions was verified at slow loading rates and subsequently a mathematical relationship was developed to relate pressure readings to volume changes. This relationship was then applied to calculate soil density changes at different stress levels.

A sandy clay agricultural soil was tested in the laboratory under triaxial conditions on an INSTRON (model 1123) testing machine. Axial load and pressure head changes were recorded on an APPLE II+ microcomputer via a 12 bit A/D converter. A data acquisition program controlled the testing machine and monitored the load and pressure transducers.

Soil samples were tested under the same moisture content (10%), initial density (1.65 g/cc), and loading rate (200 mm/min) for varying confining pressures ranging from 13.8 kPa to 41.4 kPa (2 to 6 psi). Each sample was subjected to three loading cycles and was finally allowed to fail in compression during a fourth cycle. The recorded stress levels and volume changes for the compression part of the first loading cycle of each sample were used to develop a linear relationship between stress and soil density. Additionally, the stress and strain data obtained were used to evaluate the soil parameters assuming the Mohr-Coulomb failure criterion. Consequently, these results were compared to those obtained by Brandon (1987) for the same soil and testing conditions, but different initial density.

The conclusions derived are:

- A sensitive differential pressure transducer can be used to evaluate the volume changes during a triaxial test at high loading rates.
- The initial density of the sample is affecting significantly the soil parameters. When increasing the initial density by 9%, the soil parameters (i.e. modulus of elasticity, angle of internal friction, etc.) were increased from 17% to 59%. The variation in the cohesion of the soil was attributed to the difference in specific surface between the soils used in the two studies.

# References


1. Allocca, J. A. and A. Stuart. ***Transducers theory and applications.*** Reston Publishing Co. 1984.

2. Amir, I. *et al.* 1976. Soil Compaction as a Function of Constant Pressure and Moisture. ***Con. Agr. Eng.*** 18(1):54-57.

3. Bailey, A. C. and G. E. VandenBerg. 1968. Yielding by compaction and shear in unsaturated soil. Trans. ASAE 11:307-311, 317.

4. Bailey, A. C. *et al.* 1984. Hydrostatic Compaction of Agricultural Soils. ***Trans ASAE*** 27(4):952-955.

5. Bishop, A. W. and D. J. Henkel. ***The measurement of soil properties in the triaxial test.*** E. Arnold. London, England, 1962.

6. Boilling, I. H. 1985. How to predict the Soil Compaction of Agricultural Tires. ***Int. Conf. of Soil Dynamics***, Auburn University, Alabama, vol 5, pp.936-952.

7. Bowles, J. E. ***Engineering properties of soils and their measurements.*** McGraw-Hill. 1978.

8. Brady, G. S. and H. R. Clauser. ***Materials handbook.*** McGraw-Hill. 1986.

9. Brandon, R. 1987. Constitutive relationships for agricultural soils. Unpublished Masters Thesis, VPI&SU.

10. Dunlap, W. H. and J. A. Weber. 1971. Compaction of an unsaturated soil under a general state of stress. ***Trans. ASAE*** 14:601-607.

11. Gidigasu, M. D. ***Laterite soil engineering.*** Elsevier Scientific Publishing Co. 1976.

12. Grisso, R. D., Jr. 1985. Compaction of agricultural soil by continuous deviatoric stress. Doctor of Philosophy dissertation, Auburn University, Auburn, Alabama.

13. Holman, J. P. ***Experimental methods for engineers.***, McGraw-Hill. 1978.

14. Hovanesian, J. D. and W. F. Buchele. 1959. Development of a Recording Volumetric Transducer for studying the Effects of Soil Parameters on Compaction. ***Trans ASAE*** 2(1):78-71.

15. Koolen, A. J. 1971. A Method for Soil Compactibility Determination. ***Journal Agric. Eng. Res.*** 19:271-278.

16. Koolen, A. J. and H. Kuipers. ***Agricultural soil mechanics.*** Springer-Verlag. 1983.

17. Kumar, L. and J. A. Weber. 1974. Compaction of unsaturated soil by different stress paths. Trans. ASAE 17:1064-1069, 1072.

18. Ladd, R. S. 1978. Preparing test specimens using undercompaction. Geotechnical Journal GTJODJ 1(1):16-23.

19. Lambe, T. W. ***Soil testing for engineers.*** J. Wiley and Sons, Inc. 1969.

20. Lambe, T. W. and R. V. Whittman. ***Soil Mechanics*** Wiley and Sons, Inc. 1969.

21. Larson, W. E. *et al.* 1980. Compression of Agricultural Soils from eight Soil Orders. ***Soil Sci. Soc. Amer. J.*** 44(3):450-457.

22. Pande, G. N. and O. C. Zienkiewicz. ***Soil mechanics transient and cyclic roads.*** J. Wiley and Sons. 1982.

23. Perumpral, J. V. 1969. The finite element method for predicting stress distribution and soil deformation under a tractive device. Doctor of Philosophy dissertation, Purdue University.

24. Pollock, D., Jr. 1983. Finite element analysis of multipass effect of vehicles on soil compaction. Master of Science thesis, VPI&SU, Blacksburg.

25. Rao, V. M. and J. R. Hammerle. 1973. Some Visco-elastic Properties of Hickory Clay - Ottawa Sand. ***Journal Agric. Eng. Res.*** 18:253-259.

26. Schofield, A. and P. Wroth. ***Critical state soil mechanics.*** McGraw-Hill. 1968.

27. Scott, R. and J. J. Schoustra. ***Soil mechanics and engineering.*** McGraw-Hill. 1968.

28. Soehne, W. H. 1958. Fundamentals of Pressure Distribution and Soil Compaction under Tractor Tires. ***Journal Agric. Eng. Res.*** 39(5):276-281,290.

29. Sowers, G. ***Introductory soil mechanics and foundations: Geological Engineering.*** Macmillan Publishing Co., Inc. 1979.

30. Vickers, B. ***Laboratory work in soil mechanics.*** Granada. 1983.

31. VandenBerg, G. E. 1966. Triaxial measurements of shearing strain and compaction in unsaturated soil. ***Trans. ASAE*** 5:105-107.

32. Wu, T. H. ***Soil Dynamics.*** Allyn and Bacon. Boston. 1971.

# Appendix A

## *Program Listing*

The following program was used to process the data and calculate stress, strain and density for all sampled points. The names of the files corresponding to the same experiment (i.e. first loading, first unloading, second loading ... final loading and failure) are stored in a file accessed through Unit 11 [READ (11,*)] so that the program can process the data for all loading cycles at one time. This is necessary since strain calculations depend on the absolute piston displacement from its original position and its location has to be accounted for when processing data for subsequent load cycles (i.e. strain is not equal to zero for the first point of the second compressive loading).

The file accessed through Unit 10 contains the friction data for the piston and the conditions under which they were measured. These values also need to be converted to pounds and are subtracted from the corresponding force measurement (for the same piston displacement). A flowchart of the program is shown in Figure 27.

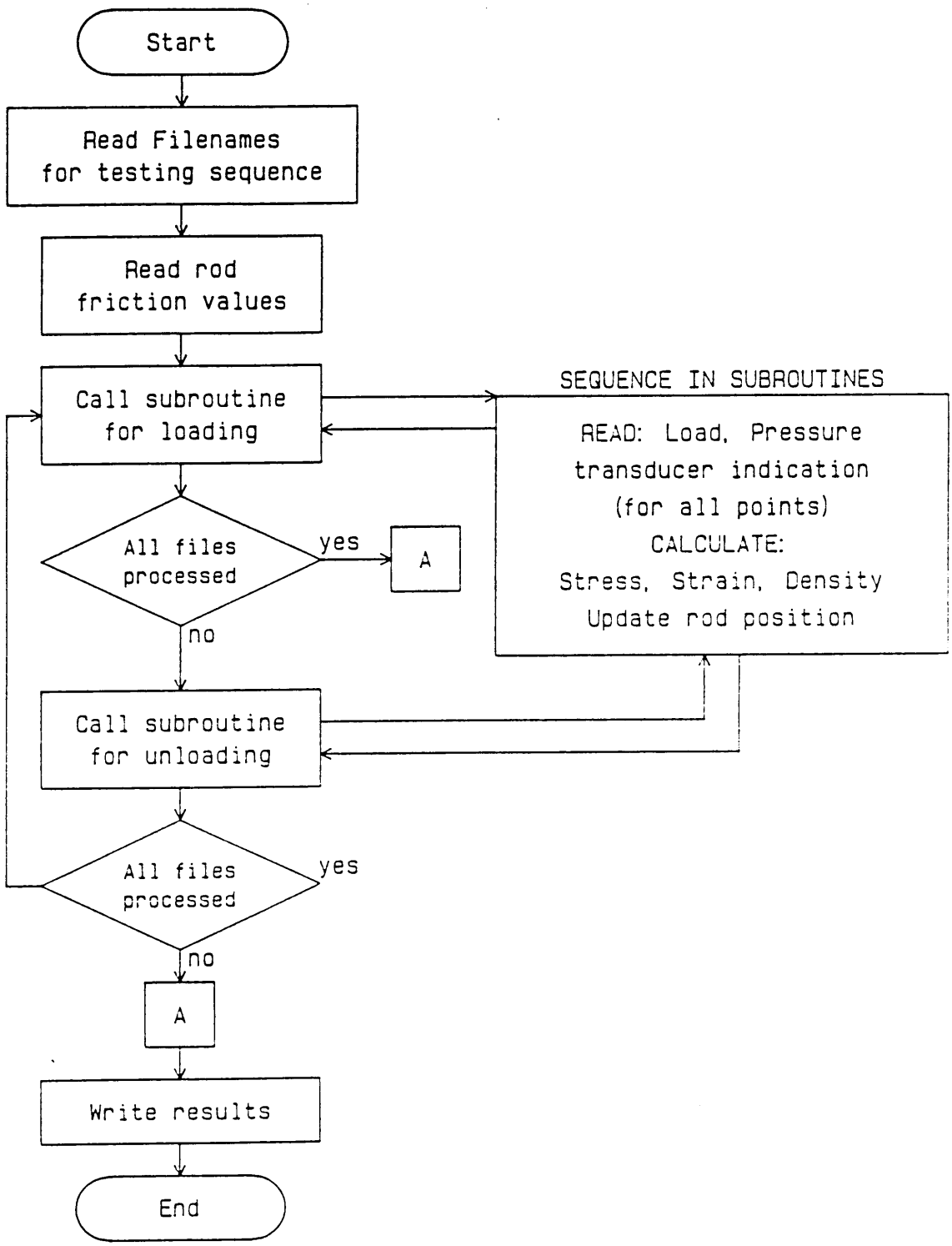


**Figure 27. Flowchart for data-reduction program**

```
C*********************************************************************
C***                                                               ***
C***     PROGRAM TO CONVERT LOAD CELL TRANSDUCER OUTPUT TO STRESS  ***
C***     AND PRESSURE TRANSDUCER OUTPUT TO VOLUME, TO CALCULATE    ***
C***     STRESS, STRAIN AND DENSITY (OR CHANGES IN DENSITY) FOR    ***
C***     EACH SAMPLE FOR THE DURATION OF THE TEST (BOTH IN         ***
C***     COMPRESSION AND IN TENSION                                ***
C***                                                               ***
C***  AREA       AREA OF SOIL SPECIMEN                             ***
C***  AC         CORRECTED AREA                                    ***
C***  FSL        FULL-SCALE LOAD ON INSTRON                        ***
C***  CH         CROSS-HEAD SPEED                                  ***
C***  ZV         ZERO-VALUE (FOR LOAD MEASUREMENTS)                ***
C***  ZV1        ZERO-VALUE (FOR D-PRESSURE MEASUREMENTS)          ***
C***  FRIC(I)    FRICTION VALUES (MEASURED IN THE BUSSHING OF THE  ***
C***             TRIAXIAL CELL.                                    ***
C***             (ZVF, CHF, FSLF ARE ASSOCIATED VARIABLES)         ***
C***  F(I)       LOAD MEASUREMENTS AND CALCULATED DEVIATORIC STRESS***
C***  V(I)       PRESSURE MEASUREMENTS AND CALCULATED VOLUME CHANGES***
C***  STRAIN(I) CORRESPONDING STRAIN VALUE                         ***
C***  FNAME(N)  NAME OF FILE WITH DATA VALUES                      ***
C***  STRIN,STROUT,LASTIN,LASTOT : DO THE HOUSEKEEPING FOR THE     ***
C***             STRAIN CALCULATIONS BETWEEN TENSION AND COMPRESSION***
C*********************************************************************
      CHARACTER *8 FNAME(8)
      COMMON  FRIC(500),FSLF,CHF,ZVF
      COMMON /CONS/PI,AREA,PISTAR,WEIGHT,SAMVOL
      PI=ARCOS(-1.0)
C PISTON AREA IN CM2
      PISTAR=2.54*2.54*PI/4.
C SAMPLE AREA (UNCORRECTED) AND SAMPLE VOLUME IN CM3  AND WEIGHT IN GR
      AREA  =PI / 4 * (2.8)**2
      SAMVOL=6 * AREA * (2.54)**3.
      WEIGHT=999.6
      READ(10,*)FSLF
      READ(10,*)CHF
      READ(10,*)ZVF
      READ(10,*,END=15) (FRIC(I),I=1,500)
   15 READ (11,*) NFIL
    1 FORMAT (A8 )
      READ (11,1) (FNAME(I),I=1,NFIL)
      WRITE(* ,*) (FNAME(I),I=1,NFIL)
      STRIN=0.
      LASTIN=1
      N=1
   10 CALL UP (FNAME(N),LASTIN,LASTOT,STRIN,STROUT)
      N=N+1
      IF (N.GT.NFIL) GOTO 99
      STRIN=STROUT
      LASTIN=LASTOT
```

```
      CALL DN (FNAME(N),LASTIN,LASTOT,STRIN,STROUT)
      N=N+1
      IF (N.GT.NFIL) GOTO 99
      STRIN=STROUT
      LASTIN=LASTOT
      GOTO 10
   99 STOP
      END
C*********************************************************************
C*  SUBROUTINE UP WILL PROCESS DATA COLLECTED DURING THE COMPRESSION
C*  TESTS. FOR THE FIRST RUN STRAIN STARTS FROM ZERO. SUBSEQUENT RUNS
C*  UTILIZE THE LAST POINT IN THE PRECEDING TENSION TEST ANALYSIS
C*  AS THE FIRST POINT IN THE COMPRESSION TEST ANALYSIS SINCE STRAINING
C*  OF THE SAMPLE DEPENDING ON PISTON TRAVEL
C*********************************************************************
      SUBROUTINE UP (FNAME   ,LASTIN,LASTOT,STRIN,STROUT)
      COMMON  FRIC(500),FSLF,CHF,ZVF
      COMMON /CONS/PI,AREA,PISTAR,WEIGHT,SAMVOL
      CHARACTER *8 FNAME
      DIMENSION F(500),STRAIN(500),ASTR(500),V(500),DDEN(500)
      INTEGER FSL,CH,ZV
      WRITE (*,*) 'UP-FNAME=',FNAME
      OPEN (9,FILE=FNAME,STATUS='OLD')
      READ(9,*)N
      READ(9,*)FSL
      READ(9,*)CH
      READ(9,*)ZV
      READ(9,*)ZV1
      J=N
      I=LASTIN
   17 READ(9,*,END=30) F(I),V(I)
      I=I+1
      GOTO 17
   30 N=I-1
      LASTOT=N
C  13 SAMPLES / SEC  RATE DETERMINED BY THE A/D CONVERTER
      DO 50 I=LASTIN,N
      STRAIN(I)=CH/(25.4*60.) * I/13.0 / 6.0
      ASTR(I)=STRAIN(I)
      AC=AREA/(1-ASTR(I))
      F(I)=((F(I)-ZV)*FSL/2048.-(FRIC(I)-ZVF)*FSLF/2048.)/AC
C CONVERT TO KPA    (1KPA=.144 PSI
      F(I)=F(I)/0.1449275
C VOL DISPLACED BY PISTON
      PISTV=I/13. *CH/60. * PISTAR  /10.
C 303 UNITS ON PRESSURE INDICATOR = 1CM3
C IF PISTV>THAN INDICATED VOLUME => SAMPLE UNDER COMPRESSION, V(I)<0
      V(I)=  ((V(I)-ZV1)/303. - PISTV)
      DDEN(I)=-WEIGHT/SAMVOL + WEIGHT/(SAMVOL + V(I))
   50 CONTINUE
```

```
      STROUT=STRAIN(N)
      WRITE (6,99)
   99 FORMAT (10X,'STRESS',9X,'STRAIN',9X,'DDEN')
      WRITE(6,100) (F(I),STRAIN(I),DDEN(I),I=LASTIN,N)
  100 FORMAT(3(5X,F10.4))
      RETURN
      END
C*********************************************************************
C*  SUBROUTINE DN WILL PROCESS DATA COLLECTED DURING THE TENSION TESTS
C*  THE FIRST POINT IS ASSIGNED THE SAME STRAIN VALUE AS THE LAST POINT
C*  IN THE PREVIOUS COMPRESSION TEST ANALYSIS.  THE LAST POINT IS
C*  SUBSEQUENTLY USED AS THE FIRST POINT IN THE FOLLOWING COMPRESSION
C*  TEST ANALYSIS
C*********************************************************************
      SUBROUTINE DN (FNAME,LASTIN,LASTOT,STRIN,STROUT)
      COMMON /CONS/PI,AREA,PISTAR,WEIGHT,SAMVOL
      DIMENSION F(500),STRAIN(500),ASTR(500),V(500),DDEN(500)
      CHARACTER *8 FNAME
      INTEGER FSL,CH,ZV
      WRITE (*,*) 'DN-FNAME=',FNAME
      OPEN (9,FILE=FNAME,STATUS='OLD')
      READ(9,*)N
      READ(9,*)FSL
      READ(9,*)CH
      READ(9,*)ZV
      READ(9,*)ZV1
C SAMPLE AREA (UNCORRECTED) AND SAMPLE VOLUME IN CM3  AND WEIGHT IN GR
      I=LASTIN
   17 READ(9,*,END=30) F(I),V(I)
      I=I-1
      IF (I.LE.0) GOTO 999
      GOTO 17
   30 N=I+1
      LASTOT=N
C  13 SAMPLES / SEC  RATE DETERMINED BY THE A/D CONVERTER
      DO 50 I=LASTIN,N,-1
      STRAIN(I)=CH/(25.4*60.) * I/13.0 / 6.0
      ASTR(I)=STRAIN(I)
      AC=AREA/(1-ASTR(I))
      F(I)=((F(I)-ZV)*FSL/2048.-15.)/AC
C CONVERT TO KPA     1KPA=.144 PSI
      F(I)=F(I)/0.1449275
C VOL DISPLACED BY PISTON (SAME AS BEFORE FOR POINT#)
      K=LASTIN-I+1
      PISTV=(K)/13. *CH/60. * PISTAR  /10.
C 303 UNITS ON PRESSURE INDICATOR = 1CM3
C IF PISTV>THAN INDICATED VOLUME => SAMPLE UNDER COMPRESSION, V(I)<0
      V(I)=   ((V(I)-ZV1)/303. - PISTV)
      DDEN(I)=-WEIGHT/SAMVOL + WEIGHT/(SAMVOL + V(I))
      STROUT=STRAIN(N)
```

```
 50 CONTINUE
    WRITE (6,99)
 99 FORMAT (10X,'STRESS',9X,'STRAIN',9X,'DDEN')
    WRITE(6,100) (F(I),STRAIN(I),DDEN(I),I=LASTIN,N,-1)
100 FORMAT(3(5X,F10.4))
    RETURN
999 WRITE (6,998)
998 FORMAT (' CAUTION!!',/
   1'TENSION TEST HAS MORE VALUES THAN COMPRESSION UP TO THIS POINT',
   2 /,'PROGRAM EXECUTION ABORTED')
    CALL EXIT
    END
```

# Appendix B

## *Calibration Data*

Representative calibration data for different loading rates

| Loading Rate [mm/min] | Number of Points | Direction | Confining Pressure [psi] | Indicated Difference [units] |
|---|---|---|---|---|
| 5 | 65 | Up | 3 | 51 |
| 5 | 65 | Up | 3 | 63 |
| 5 | 65 | Down | 3 | 50 |
| 5 | 65 | Down | 3 | 65 |
| 5 | 65 | Up | 3 | 60 |
| 5 | 104 | Up | 5 | 100 |
| 5 | 104 | Up | 5 | 118 |
| 5 | 104 | Down | 5 | 105 |
| 5 | 104 | Down | 5 | 103 |
| 50 | 26 | Up | 3 | 228 |
| 50 | 26 | Up | 3 | 239 |
| 50 | 26 | Down | 3 | 251 |
| 50 | 39 | Up | 3 | 378 |
| 50 | 78 | Down | 3 | 774 |
| 50 | 13 | Up | 5 | 102 |
| 50 | 13 | Up | 5 | 131 |
| 50 | 13 | Up | 5 | 143 |
| 50 | 26 | Down | 5 | 224 |
| 50 | 26 | Down | 5 | 269 |
| 50 | 26 | Down | 5 | 251 |
| 200 | 52 | Up | 3 | 1805 |
| 200 | 52 | Up | 4 | 1851 |
| 200 | 52 | Down | 4 | 1902 |
| 200 | 65 | Up | 5 | 2051 |
| 200 | 65 | Up | 5 | 2103 |
| 200 | 65 | Down | 5 | 2084 |
| 200 | 65 | Up | 5 | 2049 |
| 200 | 65 | Up | 5 | 2023 |

The vita has been removed from the scanned document